Biomedical Engineering Letters (2020) 10:17–41
https://doi.org/10.1007/s13534-019-00134-8

REVIEW ARTICLE

Electrochemical methods to enhance osseointegrated prostheses

Mark T. Ehrensberger[1,2] · Caelen M. Clark[1] · Mary K. Canty[1,3] · Eric P. McDermott[1]

Received: 5 May 2019 / Revised: 11 October 2019 / Accepted: 20 October 2019 / Published online: 19 November 2019

Abstract
Osseointegrated (OI) prosthetic limbs have been shown to provide an advantageous treatment option for amputees. In order for the OI prosthesis to be successful, the titanium implant must rapidly achieve and maintain proper integration with the bone tissue and remain free of infection. Electrochemical methods can be utilized to control and/or monitor the interfacial microenvironment where the titanium implant interacts with the biological system (host bone tissue or bacteria). This review will summarize the current understanding of how electrochemical modalities can influence bone tissue and bacteria with specific emphasis on applications where the metallic prosthesis itself can be utilized directly as a stimulating electrode for enhanced osseointegration and infection control. In addition, a summary of electrochemical impedance sensing techniques that could be used to potentially assess osseointegration and infection status of the metallic prosthesis is presented.

Keywords Osseointegration · Implant associated infection · Electrical stimulation · Osteogenesis · Biofilms · Electrochemical impedance spectroscopy

1 Introduction

Osseointegrated (OI) prosthetic limbs represent a promising alternative to conventional socket prosthetic limbs. The OI prostheses are directly anchored within the bone of the residual limb and utilize a percutaneous connection to the external artificial limb and terminal device. Several OI prostheses have been developed for clinical use and the design features of each implant system has recently been reviewed by Thesleff et al. [1]. The potential advantages of OI prosthetic limbs include direct load transfer to the skeleton, minimal risk of skin irritation or nerve compression, elimination of the need for prosthetic exchange due to residual limb shape changes, optimum control of the prosthetic movement, and restitution of some sensory and tactile function known as osseoperception [2]. These benefits address some of the limitations of socket prostheses and can greatly enhance the quality of life for the amputee.

In order for the OI prosthesis to be successful, it must rapidly achieve and maintain proper integration with the bone tissue and remain free of infection. Clinically it can be challenging to reliably and quantitatively assess the degree of osseointegration and the infection status of OI prostheses. Therefore, development and implementation of best clinical practices and technological innovations that can accurately assess and optimally actuate osseointegration and infection control are desirable. This review will summarize the current understanding of how electrochemical modalities can influence bone tissue and bacteria. Specific emphasis is given to applications where the OI prosthesis (or other metallic orthopedic implant) itself can be utilized directly as a stimulating electrode for enhanced osseointegration and infection control. In addition, the electrochemical impedance sensing techniques that could potentially be used to non-invasively assess osseointegration and infection status are summarized. This manuscript assumes the reader has a general understanding of basic electrochemical instrumentation and methods, details of which can be found in other reference materials [3].

✉ Mark T. Ehrensberger
mte@buffalo.edu

[1] Department of Biomedical Engineering, University at Buffalo, 445 Biomedical Research Building, 3435 Main Street, Buffalo, NY 14214, USA

[2] Department of Orthopaedics, University at Buffalo, Buffalo, NY, USA

[3] Department of Microbiology and Immunology, University at Buffalo, Buffalo, NY, USA

2 Electrochemical concepts for enhancing osseointegration

2.1 DC electrical stimulation for osteogenesis

In response to the electrical signals reported when bone was mechanically strained [4–6], the idea was put forth that endogenous electrical activity of bone may be the mediator of Wolff's law, in which bone mass maintenance and remodeling is responsive to mechanical strain. This theory spawned extensive research into the application of exogenous faradaic electrical stimulation to promote osteogenesis. The early studies by Friedenberg et al. [7–9] delivered direct current (DC) electrical stimulation to transcortical or intramedullary stainless steel cathodes in rabbits. These authors showed a dose–response relationship where optimum bone formation was reported when a constant current between 5 and 20 μA was applied.

Brighton et al. [10, 11] and Spadaro et al. [12] suggested that this faradaic enhancement of osteogenesis was linked to the reactants consumed (oxygen) and the products generated (hydroxide ion, hydrogen peroxide, and free radicals) through the electrochemical reduction of oxygen and water in the microenvironment of the cathode. Using microelectrodes to measure the pH and oxygen tension directly adjacent to intramedullary stainless steel wire cathodes in rabbits, Baranowski et al. [13, 14] showed that chronic DC electrical stimulation of 20 μA (in the current range for optimal bone formation around the cathode) produced a major depression of oxygen tension and a minor elevation in pH within the microenvironment of the cathode. It is important to highlight that the electrode current is indicative of the rate of the electrochemical reduction reaction at the cathode, but it is the electrode voltage that determines which reaction is favored to occur at the cathode. In further studies, Baranowski et al. [14, 15] generated plots of cathode voltage versus current by performing polarization studies with intramedullary stainless steel wire cathodes in rabbits. They reported three distinct regions of cathodic polarization behavior corresponding to different proposed reduction reactions at the cathode. Importantly, they also showed that these regions of polarization behavior correlated to different osteogenic responses. The current applied (20 μA) for optimal bone formation was associated with a cathodic potential of − 1.1 V versus Ag/AgCl, which fell within a polarization region where the reduction process was proposed to involve intermediate hydrogen peroxide production, oxygen consumption, and pH elevation at the cathode [14, 15]. This information is consistent with knowledge that bone growth is promoted under conditions of reduced oxygen tension [16] and elevated pH [17, 18]. Furthermore, hydrogen peroxide has been shown to stimulate secretion of vascular endothelial growth factor by macrophages [19], which is important for angiogenesis associated with bone growth/repair.

Subsequent studies emphasized that the current density and charge transfer during stimulation should be considered when optimizing the DC electrical stimulation for osteogenesis [20]. Furthermore, other studies have directly assessed the relationship between the cathode voltage and osteogenesis. Baranowski et al. [21] reported that the osteogenic response increased in direct relation to increasing stainless steel cathode potentials between − 0.6 to − 1.23 V versus Ag/AgCl and concluded that while selection of an appropriate current is important, the cathode voltage had a proportionally greater influence on osteogenesis [15, 22]. Dymecki et al. [23] reported a dose–response relationship between stainless steel wire cathode voltage and bone growth and furthermore showed that voltage-controlled DC electrical stimulation produced a greater magnitude of osteogenesis as compared to current-controlled DC electrical stimulation.

As reviewed by Griffin et al. [24], DC electrical stimulation is approved by the US Food and Drug Administration and has been utilized to enhance bone healing for several clinical applications including nonunion fractures, spinal fusion, avascular necrosis of the femoral head, and hindfoot fusion. However, while good clinical outcomes have been reported in many studies, it was recommended that more uniform and higher level of evidence clinical studies are needed to support and optimize the broad clinical implementation of DC electrical stimulation for bone healing [24].

2.2 Introduction of osseointegration

Professor Per-Ingvar Brånemark was the first to introduce the term "osseointegration" to describe the direct structural and functional connection between bone tissue and a titanium implant surface [25, 26]. Osseointegration has since been widely adopted as an effective implant fixation strategy for many dental and orthopedic applications. A recent review by Shah et al. [27] highlights the complexities of the osseointegration process that occurs at multiple length-scales. This process involves direct communication between osteocytes and the titanium implant [28, 29] and chemical integration at the nanoscale between the inorganic components of bone tissue and titanium's surface oxide film [30–33]. It is also important to note that the oxide film on titanium is dynamic and its morphology, chemistry, and interfacial electrochemical impedance have been shown to change over time with hydration in an electrolyte solution [34], with electrical polarization of the titanium substrate [34–41], and with interaction among biological species such as bone cells and inflammatory products [36, 37, 42, 43]. As summarized in a recent review by Spriano et al. [44] many

surface modification strategies have been investigated to enhance the osseointegration of titanium implants.

2.3 DC electrical simulation for enhanced osseointegration

Given the beneficial effects of DC electrical stimulation for osteogenesis described in the previous section, the application of DC electrical stimulation directly to a titanium implant has been explored as a potential approach to enhance osseointegration. Prior to reviewing these studies, it is first important to highlight fundamental differences between the use of electrical stimulation for enhancing osseointegration of titanium implants and for promoting bone healing in fractures and fusions. In bone healing applications the DC electrical stimulation is typically delivered by stainless steel wire cathodes placed near the fracture or fusion site to promote bone growth from one bone segment to another bone segment, without specific regard to the bone-electrode interface. In osseointegration applications, the DC electrical stimulation is delivered directly by a titanium implant to promote the bone growth from the surrounding bone up to surface of the implant. In this way, modulation of the interfacial electrochemical properties and biological interactions within the adjacent microenvironment of the stimulating electrode are critically important. Furthermore, the majority of osseointegrated orthopedic implants are designed for load bearing applications, whereas stimulation wires are not intended to carry load. This difference in mechanical use highlights the critical importance of promoting and maintaining a tightly integrated bone/titanium (cathode) interface for preventing micromotion and loosening of orthopedic implants during loading. Finally, it is also noteworthy that stainless steel has been used as the stimulating electrode material in the majority of bone healing applications whereas titanium implants are traditionally used for osseointegration applications. Both stainless steel and titanium are passivated metals with known biocompatibility that are used in orthopedics, however their electrochemical impedance properties and polarization behavior are different [45]. Therefore, this may indicate that the optimal electrical stimulation conditions identified for stainless steel wires to enhance bone healing might be different when applied to titanium implants for enhanced osseointegration.

2.3.1 In vitro studies (summary provided in Table 1)

While several studies have utilized in vitro methods to evaluate electrical stimulation for osteogenesis [46–52], there have also been a few relevant studies that have cultured cells directly on electrically stimulated titanium cathodes as a model to assess electrically enhanced osseointegration [38, 41, 53–57]. However, many of these studies have shown marked reductions in cell viability and morphology when osteoblasts are cultured directly on titanium that was cathodically polarized by potentiostatic methods [41, 53, 55, 57] or by galvanostatic methods [56]. Gilbert et al. [53] showed that constant cathodic polarization of titanium substrates at − 1000 mV versus AgCl for 2 h depleted oxygen from the adjacent microenvironment and reduced osteoblast spreading on the titanium. Kalbacova et al. [56] applied constant cathodic current densities of − 2.5 μA/cm^2 and − 5 μA/cm^2 to titanium substrates for 24 h and reported reductions in osteoblast viability and morphology that was associated with an increased intracellular production of reactive oxygen species. Ehrensberger et al. [41] showed an 85% reduction in viability and spreading of pre-osteoblasts cultured on titanium samples polarized at a constant cathodic potential of − 600 mV and − 1000 mV versus Ag/AgCl for 24 h. These authors proposed that voltage-dependent electrochemical thresholds (such as cathodic current density greater than − 1 μA/cm^2 and polarization resistance less than 10^5 Ω cm^2) may control the biocompatibility of titanium. Sivan et al. [57] further refined these proposed electrochemical thresholds to include time dependency and showed cell death can occur at − 400 mV versus Ag/AgCl in as little as 10 h with an associated average cathodic current density − 20 ηA/cm^2. However, Haeri et al. [55] showed that viability of cells cultured on titanium polarized at − 400 mV versus Ag/AgCl can be enhanced by pre-treatment anodization of the titanium sample. Interestingly, in contrast to the effects of constant cathodic polarization, Ciolko et al. [38] showed that 24 h of shifting the cathodic potential of titanium substrates to − 750 mV versus Ag/AgCl periodically (repeating 1 s polarization followed by 5 s of recovery at the open circuit potential) does not affect cell viability. In addition, Gittens et al. [54] showed that cathodically polarized titanium substrates enhance osteogenic differentiation of human precursor cells in a voltage-dependent manner. However, their test chamber was designed to simulate capacitive coupling electrical stimulation systems and did not allow for faradaic stimulation in the culture well.

2.3.2 In vivo studies (summary provided in Table 2)

There are several in vivo studies reported in the literature that show applying DC electrical stimulation directly to the titanium implant can enhance osseointegration [58–61]. Song et al. [61] showed in a canine mandibular model that biphasic electrical current (20 μA/cm^2, 125 μs duration, and 100 pulses/s) applied to a titanium dental implant for a duration of 7 days resulted in greater newly formed bone area and greater bone-implant contact as compared to the unstimulated controls when evaluated 2 weeks after the electrical stimulation was stopped. When evaluated after 4 weeks, the stimulated group has significantly more new bone area,

Table 1 A summary of the in vitro studies relevant to the evaluation of DC electrical stimulation effects on osseointegration

Reference	Cell type	Cathode material	Electrical configuration	Stimulation	Stimulation duration	Results
Gilbert et al. [53]	Osteoblast (rat calvaria)	cpTi (Grade 4)	Potentiostatic (3 electrode)	− 1000 mV (vs. Ag/AgCl)	2 h	Constant cathodic polarization of titanium substrates depleted oxygen from the adjacent microenvironment and reduced osteoblast spreading on the titanium
Kalbacova et al. [56]	Osteoblast (MG63)	Ti–6Al–4V (ASTM 136)	Galvanostatic (2 electrode)	$-2.5\ \mu A/cm^2$ $-5\ \mu A/cm^2$	24 h	Reductions in osteoblast viability and morphology that was associated with an increased intracellular production of reactive oxygen species
Ehrensberger et al. [41]	Pre-osteoblast (MC3T3-E1)	cpTi (Grade 4)	Potentiostatic (3 electrode)	− 600 mV − 1000 mV (vs. Ag/AgCl)	24 h	85% reduction in viability and spreading of pre-osteoblasts cultured on titanium samples when polarized at a constant cathodic potential
Sivan et al. [57]	Pre-osteoblast (MC3T3-E1)	Ti–6Al–4V (ASTM F136)	Potentiostatic (3 electrode)	− 400 mV (vs. Ag/AgCl) [~ $20nA/cm^2$]	10 h	Cell death can occur at in as little as 10 h with an associated average cathodic current density of − 20 ηA/cm^2
Haeri et al. [55]	Pre-osteoblast (MC3T3-E1)	cpTi (Grade 4)	Potentiostatic (3 electrode)	− 400 mV (vs. Ag/AgCl)	24 h	Viability of cells cultured onto polarized titanium can be enhanced by pre-treatment anodization of the titanium sample
Ciolko et al. [38]	Pre-osteoblast (MC3T3-E1)	cpTi (Grade 2)	Shifting Cathodic Potential (3 electrode)	− 750 mV (vs. Ag/AgCl)	24 h (1 s on, 5 s off)	Cell viability was not affected by periodic cathodic shifting of the potential of titanium substrates
Gittens et al. [54]	Osteoblast (MG63)	cpTi (Grade 2)	Potentiostatic (2 electrode)	− 100 mV	2 h	Cathodically polarized titanium substrates enhance osteogenic differentiation of human pre-cursor cells in a voltage-dependent manner

Table 2 A summary of the in vivo studies relevant to the evaluation of DC electrical stimulation effects on osseointegration

Reference	Animal model	Implant material	Electrical configuration	Stimulation	Stimulation duration	Results
Song et al. [61]	Canine (Mandibular)	Titanium Dental Implant	Biphasic current (2 electrode)	20 μA/cm^2 [125 μs pulse, 100 pulses/s]	7 days	Significant increase in newly formed bone area (2 and 4 weeks post stimulation) and bone-implant contact (2 weeks post stimulation)
Colella et al. [59]	Canine (Tibia)	Porous Titanium cylinder (Cathode)	Galvanostatic (2 electrode)	15 μA (~48 μA/cm^2)	1–8 days	Significant increase in the interfacial shear strength during push out testing conducted post-implantation
Bins-Ely et al. [58]	Canine (Tibia)	cpTi [Grade 4] (Anode)	Galvanostatic (2 electrode)	10 μA (~3.6 μA/cm^2) 20 μA (~7.2 μA/cm^2)	7 and 15 days	Significantly higher bone-implant interface contact area for the 20 μA condition as compared to the 10 μA and control conditions at 15 days; No significant difference at the 7-day conditions
Shayesteh et al. [60]	Canine (Mandibular)	Titanium dental implant	Potentiostatic (2 electrode)	3 V 20 μA (~5 μA/cm^2)	30 days	Significant increase in bone contact ratio and local bone formation around the stimulated implants as compared to unstimulated control implants when evaluated at 90 days
Dergin et al. [62]	Sheep (Tibia)	Titanium dental implant (Cathode)	Galvanostatic (2 electrode)	7.5 μA (~2.75 μA/cm^2)	4, 8, and 12 weeks (12 h/day)	No significant increase in bone-implant contact ratio, osteoblast activity, or new bone formation as compared to controls
Shafer et al. [64]	Rabbit (Mandibular)	Titanium dental implant (Cathode)	Galvanostatic (2 electrode)	7.5 μA (~2.5 μA/cm^2)	28 days	No significant enhancement of removal torque or increased percentage of bone adjacent to the implant
Isaacson et al. [63]	Rabbit (Femur, Intramedullary)	Gold-coated Ti–6Al–4V (Cathode)	Potentiostatic (2 electrode)	0.55 V	3 and 6 weeks	No significant enhancement of appositional bone index and mineral apposition rates; There was an increase in trabecular bone around the stimulated implants

however, there were no differences in bone-implant contact area between the groups [61]. Colella et al. [59] reported that compared to unstimulated controls, a constant current of 15 μA (~48 μA/cm^2, based upon estimated surface area of 0.31 cm^2) applied for 1–8 days to a porous titanium cylinder cathode implanted in the cortical bone of a canine tibiae increased the interfacial shear strength during push out testing conducted at 1, 2, and 3 weeks post-implantation. Based upon the mechanical outcomes it was suggested that the rate and quantity of bone ingrowth were enhanced by electrical stimulation [59]. Bins-Ely et al. [58] applied constant current of 10 μA (~3.6 μA/cm^2) or 20 μA (~7.2 μA/cm^2) for 7 and 15 days to titanium dental implants (connected as anode to the + terminal of the power source) placed in the cortical bone of canine tibiae. They found significantly higher bone-implant interface contact area for the 20 μA condition as compared to the 10 μA and control conditions at 15 days. However, there were no differences noted between the groups at 7 days [58]. Utilizing a canine mandibular model Shayesteh et al. [60] enforced a 3 V difference between two titanium dental implants (assumed to generate a constant 20 μA or ~5 μA/cm^2) for 30 days and reported an increased bone contact ratio and increased local bone formation around the stimulated implants as compared to unstimulated control implants when evaluated at 90 days. The authors did not specify whether the stimulated implants evaluated were the anode or cathode.

However, there are also a few in vivo studies that showed DC electrical stimulation does not enhance osseointegration of titanium implants [62–64]. Dergin et al. [62] showed that a constant current of 7.5 μA (~2.75 μA/cm^2) applied for 12 h per day to titanium dental implants (cathode) placed in sheep tibiae for 4, 8, and 12 weeks did not increase bone-implant contact ratio, osteoblast activity, or new bone formation as compared to controls. Utilizing a rabbit mandibular model, Shafer et al. [64] reported that a constant current of 7.5 μA (~2.5 μA/cm^2) applied to titanium dental implants (cathodes) for 28 days showed no enhancement of removal torque or increased percentage of bone adjacent to the implant. Isaacson et al. [63] applied a potential difference of 0.55 V between a gold-coated titanium rod (cathode) placed in the intramedullary canal of rabbit femur and an identical rod (anode) placed in the adjacent musculature. Histological assessment following stimulation periods of 3 and 6 weeks did not show an electrical enhancement of appositional bone index and mineral apposition rates, however the authors did note an increase in trabecular bone around the stimulated implants [63].

2.3.3 Discussion

While there are seemingly disparate in vivo outcomes reported for using DC electrical stimulation to enhance osseointegration [58–64], there are a few important aspects to highlight. First, these studies did not utilize a uniform protocol and the differences in the DC electrical stimulation applied (magnitude, duration, pattern, control unit), animal model used (dog, rabbit, sheep), experimental timeline (stimulation durations relative assessment time points), implant type (threaded titanium dental implant, porous titanium cylinder, gold-coated titanium rod), and implant location (mandible, femur, tibia, transcortical, intramedullary) all may contribute to the differences in the reported outcomes. However, there are a couple of consistent features in all studies that showed the electrical stimulation was beneficial. For example, electrical enhancement was shown in canine models with current densities greater than ~5 μA/cm^2. It is also important to emphasize that the majority of these studies have employed a current-controlled DC electrical stimulation to deliver a constant amperage to the titanium cathode instead of using a voltage-controlled DC electrical stimulation to deliver a constant voltage to the titanium cathode, which has been previously suggested for optimal osseous response [15, 21–23]. Isaacson et al. [63] utilized a two-electrode, potential difference electrical stimulation method, however, they did not measure the current density during the experiment and therefore, were unable to quantify the faradaic stimulation processes and the relationship it had with the bone response. Furthermore, the stimulation system of Isaacson et al. [63] did not utilize a reference electrode, and therefore was likely unable to maintain/control the absolute potential of the implant and thus unable to precisely modulate the voltage-dependent electrochemical processes at the interface [39–41, 65]. A recently developed cathodic voltage-controlled electrical stimulation (CVCES) method [66], which utilizes a three-electrode potentiostatic configuration to precisely maintain the absolute voltage of the working electrode (titanium cathode) with respect to a stable reference electrode, may find utility for voltage-controlled stimulation of titanium cathodes for enhanced osseointegration.

Another interesting point to emphasize is that cathodic current densities greater than ~5 μA/cm^2 were shown to be beneficial in vivo, but current densities of that magnitude were detrimental in vitro. This may indicate that cell culture studies using freshly seeded osteoblasts on polarized titanium may not adequately model the complexities of the in vivo situation which may govern the effects that DC electrical stimulation has on the in vivo cellular response. For example, the simplified cell culture model does not account for inflammatory or immune responses, bone remodeling (osteoblast-osteoclast interplay), or the role of mechanotransduction. Furthermore, in vivo the mineralized extracellular matrix may also have a role in the spatial distribution and effects of the DC electrical stimulation.

2.4 Future directions

While DC electrical stimulation is used clinically for enhancing fracture healing and bone fusions, it has not been utilized clinically for enhancing osseointegration of titanium implants. In order to move towards clinical use, future studies assessing electrically enhanced osseointegration will need to establish more robust in vitro models or identify a uniform in vivo model that could be utilized as a testbed to identify optimal stimulation parameters. In addition, if the goal is to evaluate the utility of electrical stimulation to enhance osseointegration for OI prosthetic limbs or joint replacement applications, it will be necessary to conduct the studies with an in vivo model that utilizes intramedullary implants. Ideally these models would also be load bearing to account for the role of mechanical stimuli [67].

3 Electrochemical concepts for enhancing infection control

The use of DC electrical stimulation for infection control has been reported in the literature utilizing a wide variety of experimental protocols. Many of these studies focused on using DC electrical stimulation as a treatment to eradicate established infections or remove adherent bacteria from surfaces [65, 68–98], while only a few focused on using the stimulation to prevent bacterial attachment and the establishment of infections [69, 99–103]. Different modes of DC electrical stimulation have also been tested, including both current-controlled DC electrical stimulation [30, 72–74, 76, 77, 79–82, 86, 88, 94–98, 101, 103–105] and voltage-controlled DC electrical stimulation [65, 68, 69, 71, 75, 83–85, 87, 89, 91–93, 99, 100]. Many of these studies have evaluated the antimicrobial effects of DC electrical stimulation by placing stimulating electrodes in proximity of bacterial biofilms formed on adjacent surfaces of interest [73–75, 77, 79, 81, 82, 88, 90, 92, 93, 96–98, 101, 104, 105]. Other studies have assessed how DC electrical stimulation effects bacteria cultured directly on the stimulating electrodes [65, 68–72, 80, 85–87, 89, 94, 95, 99, 100, 103]. In addition, the effects of DC electrical stimulation have been explored as a stand-alone antimicrobial treatment [65, 69, 71, 72, 74–76, 79, 80, 83, 85–92, 94, 95, 99–101, 103, 104] or in combination with antibiotics and disinfectants [68–70, 73, 77, 81–84, 88, 93, 96–98, 105]. Furthermore, the majority of studies evaluating the antimicrobial effects of DC electrical stimulation report in vitro outcomes only, however a few in vivo studies have also been performed [65, 72, 83, 84, 103]. The focus of this review will be on those studies that have evaluated the effects of DC electrical stimulation on clinically-relevant bacteria that were directly associated with the surface of stimulating electrodes composed of implant alloys utilized in orthopedics. A review of these specific studies will be presented first, followed by broad discussion of concepts proposed to explain the possible mechanism of DC electrical stimulation for infection control.

3.1 In vitro evaluations of bacteria on stimulating electrodes (summary provided in Table 3)

Utilizing a parallel plate flow chamber, van der Borden et al. [94, 95, 106] has reported on the effects of current-controlled electrical stimulation to cause detachment of *Staphylococcus epidermidis* (*S. epidermidis*)from stainless steel substrates (cathodes). It was shown that an application of 100 μA (4.76 μA/cm^2) for 150 min caused an average detachment of 54% of initially adherent *S. epidermidis* (strain HBH276) from stainless steel [106], whereas electric block currents of 100 μA (4.76 μA/cm^2, 25–50% duty cycle, 0.1–2 Hz) showed an increased average detachment of 76% under the same experimental conditions [94]. The same authors also evaluated the influence of electrical stimulation on the detachment of established biofilms of *S. epidermidis* on stainless steel. In this study, application of 100 μA (4.76 μA/cm^2) for 360 min caused an average detachment of 78% of biofilm associated bacteria, while 100 μA (4.76 μA/cm^2) electric block current (50% duty cycle, 1 Hz) yielded only 31% detachment [95]. These reports also indicated that the electrical currents reduced viability of the bacteria that remained on the stainless steel [94, 95].

Rabinovitch et al. [87] showed that connecting stainless steel coupons to the negative terminal of a 6-volt battery for 30 s can physically disrupt preformed biofilms of *S. epidermidis* and reduce the number of surface-associated viable bacteria by four orders of magnitude. They hypothesized that these effects were due to the increased pH causing alkaline hydrolysis of the polysaccharide biofilm matrix and hydrogen gas bubble evolution physically pushing the biofilm away from the stainless steel substrate [87]. Dargahi et al. [71] showed that *Pseudomonas aeruginosa* (*P. aeruginosa*) biofilms could be removed from stainless steel substrates upon cathodic polarization greater than − 1.5 V versus Ag/AgCl and proposed that hydrogen gas evolution was the primary mechanism responsible for the removal.

Costerton et al. [70] showed synergistic reductions of *P. aeruginosa* biofilms on stainless steel substrates when electrical stimulation was combined with antibiotic therapy. These authors used a flow cell in which the polarity of adjacent stainless steel electrodes alternated every 64 s with an average current density of 1.7 mA/cm^2. Application of this electrical stimulation pattern for 48 h in the presence of five times the minimal inhibitory concentration (MIC) of tobramycin produced an almost complete kill of *P. aeruginosa* biofilms preformed on the stainless steel [70]. The authors proposed that electrically assisted

Table 3 A summary of the in vitro studies that evaluated effects of electrical stimulation on bacteria that were cultured directly on the stimulating electrode

Reference	Stimulation type	Electrical configuration	Electrode materials*	Stimulation parameters	Bacteria	Results
van der Borden et al. [106]	Current-controlled	Two electrodes connected to a constant current source and placed in a parallel plate flow chamber with potassium phosphate buffer	Stainless steel (WE) Indium-tin-oxide (CE)	15 or 100 µA applied for 2.5 h	*Staphylococcus epidermidis* initially adhered to stainless steel	Application of 100 µA for 150 min caused an average detachment of 54% of initially adherent bacteria from stainless steel cathodes
van der Borden et al. [94]	Current-controlled	Two electrodes connected to a constant current source and placed in a parallel plate flow chamber with phosphate buffered saline	Stainless steel (WE) Indium-tin-oxide (CE)	15, 60, or 100 µA block currents (5–50% duty cycle at 0.1–2 Hz) applied for 2.5 h	*Staphylococcus epidermidis* initially adhered to stainless steel	Application of electric block currents of 100 µA (25–50% duty cycle, 0.1–2 Hz) caused an average detachment of 76% of initially adherent bacteria from stainless steel cathodes
van der Borden et al. [95]	Current-controlled	Two electrodes connected to a constant current source and placed in a parallel plate flow chamber with phosphate buffered saline	Stainless steel (WE) Indium-tin-oxide (CE)	60 or 100 µA either DC or block current (50% duty cycle at 1 Hz) for 360 min	*Staphylococcus epidermidis* biofilms preformed on electrodes	Application of 100 µA for 360 min caused an average detachment of 78% of biofilm associated bacteria, while 100 µA electric block current (50% duty cycle, 1 Hz) yielded only 31% detachment
Rabinovitch et al. [87]	Voltage-controlled	Two electrodes connected to 6 V battery and placed in a beaker or dish filled with saline	Stainless steel	6 V applied from 10 s to 5 min	*Staphylococcus epidermidis* biofilms preformed on electrodes	Electrodes connected to the negative terminal of the battery for 30 s had physically disrupted biofilms and reduced the amount of surface-associated viable bacteria by four orders of magnitude
Dargahi et al. [71]	Voltage-controlled	Three electrodes connected to a potentiostat and placed in unspecified chamber filled with phosphate buffered saline	Stainless steel (WE) Graphite (CE) Ag/AgCl (RE)	− 0.5 V to − 3.0 V for up to 60 s	*Pseudomonas aeruginosa* biofilms pre-formed on stainless steel electrodes	Cathodic polarization greater than − 1.5 V versus Ag/AgCl for 60 s or less removed the biofilms

Table 3 (continued)

Reference	Stimulation type	Electrical configuration	Electrode materials*	Stimulation parameters	Bacteria	Results
Costerton et al. [70]	Current-controlled	Three electrodes connected to a direct current generator and placed into a flow cell with culture media	Stainless steel	polarity of adjacent electrodes alternate every 64 s with an average current density of 1.7 mA/cm^2	*Pseudomonas aeruginosa* biofilms pre-formed on stainless steel electrodes	Application of this electrical stimulation pattern for 48 h in the presence of five times the minimal inhibitory concentration of tobramycin produced an almost complete kill of *P. aeruginosa* biofilms preformed on the stainless steel
Mohn et al. [80]	Current-controlled	Two electrodes connected to an unspecified electric circuit. Electrodes separated by electrically conductive ballistics gel	Titanium dental implants	2, 5, 7.5, 10 mA for 15 min	*Escherichia coli* biofilms pre-formed on electrodes	7.5 mA and 10 mA completely killed all bacteria at the anode and reduced viable bacteria by two orders of magnitude at the cathode
Schneider et al. [89]	Voltage-controlled	Two electrodes connected to a potentiostat. Electrodes separated in an electrolysis chamber	Titanium dental implants (cathode) and platinum (anode)	7.0 V and 300 mA for 30 s	Mixed species wildtype biofilms pre-formed on titanium electrode	Bacterial biofilm was completely removed from a titanium dental implant (cathode) upon application of optimized electrolysis stimulation of 30 s at 7.0 V and 300 mA
Ehrensberger et al. [65]	Voltage-controlled	Three electrodes connected to a potentiostat. Electrodes were immersed in saline and separated by electrically conductive agar	Titanium (WE) Graphite (CE) Ag/AgCl (RE)	− 1.8 V for 1 h	Methicillin-resistant *Staphylococcus aureus* biofilms pre-formed on titanium electrode	Application of − 1.8 V for 1 h significantly reduced the CFU enumerated from the pre-formed biofilm on the titanium by 97% and from the planktonic bacteria in the surrounding solution by 92%
Canty et al. [100]	Voltage-controlled	Three electrodes connected to a potentiostat. Electrodes were immersed in culture media and separated by electrically conductive agar	Titanium (WE) Graphite (CE) Ag/AgCl (RE)	− 1.5 V or − 1.8 V for 2, 4, 8 h	Methicillin-resistant *Staphylococcus aureus* or *Acinetobacter baumannii* planktonic	No detectable titanium coupon-associated or planktonic CFU for either MRSA or *A. baumannii* were enumerated following − 1.8 V for 8 h. Applying − 1.8 V for 4 h reduced titanium coupon-associated MRSA and *A. baumannii* CFU by 99.9% and reduced planktonic CFU below detectable levels for both strains

Table 3 (continued)

Reference	Stimulation type	Electrical configuration	Electrode materials*	Stimulation parameters	Bacteria	Results
Canty et al. [69]	Voltage-controlled	Three electrodes connected to a potentiostat. Electrodes were immersed in culture media and separated by electrically conductive agar	Titanium (WE) Graphite (CE) Ag/AgCl (RE)	− 1.0 V, − 1.5 V, or − 1.8 V for 24 h	Methicillin-resistant *Staphylococcus aureus* or *Pseudomonas aeruginosa* planktonic and biofilms pre-formed on titanium electrode	Applying − 1.8 V for 24 h eradicates MRSA and *P. aeruginosa* biofilms pre-formed on titanium surfaces. Synergistic reductions in MRSA and *P. aeruginosa* biofilms when CVCES at − 1.5 V was delivered to the titanium for 24 h in combination with clinically relevant antibiotics. 24 h of CVCES at − 1.5 V in combination with antibiotic prophylaxis was able to prevent MRSA and *P. aeruginosa* attachment on titanium coupons

*Note that *WE* is the working electrode, *CE* is the counter electrode, and *RE* is the reference electrode

electrophoresis was responsible for this bioelectric effect, with perhaps additional contributions from an electrochemically generated agent that enhances the antibiotic effect [70].

Mohn et al. [80] applied current-controlled stimulation of 2 to 10 mA (~ 0.5 to 2.5 mA/cm^2) for 15 min between a pair of titanium dental implants that were embedded into conductive ballistic gel and had performed biofilms of *Escherichia coli* (*E. coli*) on their surfaces. They showed that constant currents of 7.5 mA (~ 1.8 mA/cm^2) and 10 mA (~ 2.5 mA/cm^2) had a robust antimicrobial effect that completely killed all bacteria at the anode and reduced viable bacterial by two orders of magnitude at the cathode [80]. These authors reported rapid and pronounced changes in pH around the physically separated anode site (pH ~ 2) and the cathode site (pH ~ 12) and suggested these electrochemically driven changes were associated with the antimicrobial outcomes [80]. Schneider et al. [89] has reported that a 14-day old wildtype mixed species bacterial biofilm was completely removed from a titanium dental implant (cathode) upon application of optimized electrolysis stimulation of 30 s at 7.0 V and 300 mA(~ 77 mA/cm^2). It was proposed the antimicrobial effects were due to hydrogen gas evolution lifting the biofilms off the surface in combination with electrochemically generated oxidants and changes in pH [89].

Ehrensberger et al. [65] explored cathodic voltage-controlled electrical stimulation (CVCES) of titanium as an antimicrobial strategy to eradicate established bacterial biofilms of methicillin-resistant *Staphylococcus aureus* (MRSA). The authors reported that compared to the open circuit potential (OCP) control conditions, application of CVCES at − 1.8 V versus Ag/AgCl for 1 h significantly reduced the colony-forming units (CFU) of MRSA enumerated from a pre-formed biofilm on the titanium by 97% and from the planktonic bacteria in the surrounding solution by 92% [65]. Further, Canty et al. [100] showed that CVCES prevents MRSA and *Acinetobacter baumannii* (*A. baumannii)* from colonizing titanium coupons and eradicates the surrounding planktonic bacteria in a magnitude- and time-dependent manner. In general, CVCES at − 1.8 V versus Ag/AgCl was found to produce more robust antimicrobial effects than CVCES at − 1.5 V versus Ag/AgCl, and this effect was enhanced as the duration of stimulation was increased. Remarkably, no detectable coupon-associated or planktonic CFU for either MRSA or *A. baumannii* were enumerated following CVCES of − 1.8 V versus Ag/AgCl for 8 h [100]. Compared to no treatment controls, CVCES at − 1.8 V for 4 h significantly reduced coupon-associated MRSA and *A. baumannii* CFU by 99.9% and reduced planktonic CFU below detectable levels for both strains [100]. Furthermore, increasingly cathodic levels of CVCES were associated with an alkaline shift in pH, a likely contributing factor in the observed antimicrobial effect [100].

Canty et al. [69] has also recently reported that extending the duration of CVCES at − 1.8 V versus Ag/AgCl to 24 h effectively eradicates MRSA and *P. aeruginosa* biofilms preformed on titanium surfaces. These authors also reported significant and synergistic reductions in MRSA and *P. aeruginosa* biofilms when CVCES at − 1.5 V versus Ag/AgCl was delivered to the titanium for 24 h in combination with clinically relevant antibiotics [69]. Furthermore, it was shown that 24 h of CVCES at − 1.5 V versus Ag/AgCl in combination with antibiotic prophylaxis was able to completely prevent MRSA and *P. aeruginosa* attachment on titanium coupons [69]. The exact mechanism governing the CVCES antimicrobial effects are unknown but are postulated to involved faradaic modification of the surrounding microenvironment that includes alkaline shifts in pH and other electrochemically generated species at the cathode.

3.2 In vivo evaluations of bacteria on stimulating electrodes (summary provided in Table 4)

Importantly, there have also been a few in vivo studies that have utilized an orthopedic implant as a stimulating electrode for infection control. Utilizing a goat model, van der Borden et al. [103] reported that delivery of a constant current of 100 µA for 21 days to stainless steel external fixation pins (cathode) was able to prevent *S. epidermidis* pin site infections from developing in 89% of the sites evaluated. Del Pozo et al. [101] utilized a rabbit model of osteomyelitis with *S. epidermidis* to show that applying constant current of 200 µA (~ 78 µA/cm^2) to an intramedullary stainless steel rod (cathode) for 21 days produced a significant 1.5 order of magnitude reduction in the bacterial burden as compared to treatment with only doxycycline. These authors also reported discoloration of the bones that were exposed to the prolonged electrical current, however, there was no further histology reported [101]. Utilizing a rodent model of an established MRSA implant-associated infection, Ehrensberger et al. [65] reported that a 1 h application of CVCES at − 1.8 V versus Ag/AgCl significantly reduced the CFU of MRSA enumerated from the bone tissue by 87% and a titanium implant by 98% when assessed immediately following the stimulation as compared to OCP controls. A subsequent study by Nodzo et al. [83], using the same rodent implant infection model, showed that bacteria which survived the initial CVCES (− 1.8 V/1 h) were able to re-establish the infection when assessed 1 week post-stimulation. However, combining the initial CVCES (− 1.8 V/1 h) with a 1-week time course of vancomycin produced a 99.8% reduction of the bone and implant bacterial burden as compared to the no treatment control animals [83]. Furthermore, additional work by Nodzo et al. [84] reported that when the initial CVCES (− 1.8 V/1 h) was combined with a prolonged 5-week course of vancomycin, remarkably, 80% of the animals had no MRSA CFU detectable on the implant nor bone tissue. This was in contrast to the prevalent bacterial burden present on the implant and in the bone tissue for animals in the no treatment control group and those animals that received the prolonged vancomycin without CVCES [84]. Importantly, in all of these reported CVCES animal studies, no deleterious histological changes or necrosis of the adjacent bone tissue was observed [65, 83, 84].

3.3 Proposed antimicrobial mechanisms

Many theories have been generated to describe the proposed mechanisms of action governing the antimicrobial effects associated with DC electrical stimulation [107–109]. These proposed mechanisms can broadly be categorized as those that are solely electrochemical in origin (faradaic effects) and those that combine electrochemical processes with antibiotics or biocides (bioelectric effect). Each of these categories is further summarized below.

3.3.1 Faradaic effects

The faradaic effects are associated with the reactants consumed and the products generated in the electrochemical reduction reactions at the cathode and the oxidation reactions at the anode. The cathodic processes can involve the reduction of oxygen and water and the production of hydroxide (alkalization), hydrogen gas, and hydrogen peroxide. The anodic processes can include the oxidation of water and chloride ion and the generation of oxygen, protons (acidification), and hypochlorous acid. Unfortunately, most reported studies assessing DC electrical stimulation have been conducted where the anode and cathode are both immersed within the same test chamber making it difficult to clearly differentiate the independent antimicrobial effects of the anodic and cathodic processes. However, a few studies have utilized test chambers designed to physically separate the anode and cathode with agar or conductive membranes [65, 69, 80, 89, 100]. This approach still allows for electrical conduction between the electrodes, but isolates the chemical reactions that cause microenvironmental changes around the cathode and anode. These studies report that both the cathodic and anodic processes can have antimicrobial effects [65, 69, 80, 89, 100]. However, in the clinical context of applying electrical stimulation directly to an orthopedic device for infection control, the implant will function as either an isolated cathode or an isolated anode. Implementation of cathodic stimulation may be clinically advantageous given that it has shown promise for enhanced bone healing and osseointegration. Therefore, the subsequent discussion will focus only on the antimicrobial mechanisms proposed for cathodic processes.

Table 4 A summary of the in vivo studies that evaluated effects of electrical stimulation on bacteria that were cultured directly on the stimulating electrode

References	Animal model	Bacteria	Stimulation type	Electrical configuration	Electrode materials*	Treatment parameters	Results
van der Borden et al. [103]	Goat tibia model of external fixation pin track infection	*Staphylococcus epidermidis* pin site inoculation	Current-controlled	Two electrodes connected to an external constant current source	Stainless steel external fixation pin (cathode), and platinum ring (anode) placed on skin	Constant current of 100 µA for 21 days	Constant current of 100 µA for 21 days to stainless steel external fixation pins (cathode) was able to prevent *S. epidermidis* pin site infections from developing in 89% of the sites evaluated
Del Pozo et al. [101]	Rabbit tibia model of osteomyelitis	*Staphylococcus epidermidis* biofilm formed on stainless steel	Current-controlled	Two electrodes connected to an external constant current source	Stainless steel intramedullary rod (cathode) and stainless steel wire (anode) wrapped around bone	Constant current of 200 µA for 21 days	Applying constant current of 200 µA to an intramedullary stainless steel rod (cathode) for 21 days produced a significant 1.5 order of magnitude reduction in the bacterial burden as compared to treatment with only doxycycline. Discoloration of the bones that were exposed to the prolonged electrical current was reported
Ehrensberger et al. [65]	Rodent shoulder model of implant associated infection	Methicillin-resistant *Staphylococcus aureus* biofilm formed on titanium electrode	Voltage-controlled	Three electrodes connected to an external potentiostat	Titanium rod (WE) implanted through humeral head; Platinum wire (CE) and sintered Ag/AgCl (RE) placed in adjacent soft tissue	− 1.8 V for 1 h	Applying − 1.8 V for 1 h significantly reduced the CFU of MRSA enumerated from the bone tissue by 87% and a titanium implant by 98% when assessed immediately following the stimulation as compared to OCP controls. Histology showed stimulation had no deleterious effect of the bone tissue

Table 4 (continued)

References	Animal model	Bacteria	Stimulation type	Electrical configuration	Electrode materials*	Treatment parameters	Results
Nodzo et al. [83]	Rodent shoulder model of implant associated infection	Methicillin-resistant *Staphylococcus aureus* biofilm formed on titanium electrode	Voltage-controlled	Three electrodes connected to an external potentiostat	Titanium rod (WE) implanted through humeral head; Platinum wire (CE) and sintered Ag/AgCl (RE) placed in adjacent soft tissue	− 1.8 V for 1 h ± 1 wk of vancomycin dosing	Combining the application of − 1.8 V for 1 h with a 1-week time course of vancomycin produced a 99.8% reduction of the bone and implant bacterial burden as compared to the no treatment control animals. Histology showed stimulation had no deleterious effect of the bone tissue
Nodzo et al. [84]	Rodent shoulder model of implant associated infection	Methicillin-resistant *Staphylococcus aureus* biofilm formed on titanium electrode	Voltage-controlled	Three electrodes connected to an external potentiostat	Titanium rod (WE) implanted through humeral head; Platinum wire (CE) and sintered Ag/AgCl (RE) placed in adjacent soft tissue	− 1.8 V for 1 h ± 5 wk of vancomycin dosing	Combining the application of − 1.8 V for 1 h with a prolonged 5-week course of vancomycin, remarkably, 80% of the animals had no MRSA CFU detectable on the implant nor bone tissue. This was in contrast to the prevalent bacterial burden present on the implant and in the bone tissue for animals in the no treatment control group and those animals that received the prolonged vancomycin without CVCES. Histology showed stimulation had no deleterious effect of the bone tissue

*Note that *WE* is the working electrode, *CE* is the counter electrode, and *RE* is the reference electrode

The oxygen and water reduction reactions produce hydroxide which can result in a local alkaline environment around the cathode. The microenvironment pH can influence the bacterial surface charge by promoting the dissociation or protonation of the bacterial cell surface functional groups [110]. At physiological pH it has been reported that most bacteria have a negative surface charge [110]. Therefore, electrostatic repulsive forces likely exist between the negatively charged bacteria and a negatively charged cathode surface. Stoodley et al. [91] showed mixed species biofilms of *Klebsiella pneumoniae*, *Pseudomonas fluorescens*, and *P. aeruginosa* biofilms expanded 4% when the platinum wire substrate was cathodically polarized. Furthermore, as highlighted by Poortinga et al. [85, 86], an alkaline pH surrounding a stimulating cathode may cause the bacteria and electrode surfaces to become more negatively charged and further promote bacterial detachment from the cathode surface. In addition, the extracellular polymeric substances (EPS) that create the matrix of a bacterial biofilm also contain negatively charged functional groups which contribute to the expansion of biofilm structures on wires that were polarized as cathodes [91]. Further, Sweity et al. [111] showed that increased pH levels can cause the EPS to stretch due to its negatively charged functional groups. Consequentially, cathodic electrochemical processes on the electrode surface that increase the local pH can also be acting to disrupt the central components for biofilm matrix formation or stability.

Previous studies have reported on the relationship between bacterial viability and the microenvironment pH following application of electrical stimulation within various experimental setups [69, 74, 80, 88, 100]. Del Pozo et al. [74] showed the application of low-intensity electric current via two stainless steel electrodes for 7 days was shown to increase the media pH (~ 12) and decrease bacterial CFU of adjacent biofilms of *Staphylococcus aureus, S. epidermidis,* and *P. aeruginosa* exposed to the treatment. Similarly, Mohn et al. [80] reported decreased CFU of *E. coli* biofilms grown directly on titanium cathodes exposed to direct current densities (− 0.5 to − 2.5 mA/cm^2) that increased the microenvironment pH (~ 12). An elevated pH (~ 9) and an increased killing of *S. epidermidis* biofilms adjacent to the platinum cathode was reported by Sandvik et al. following the application of direct current densities (− 0.7 to − 1.8 mA/cm^2) for 24 h [88]. Canty et al. [100] reported that application of − 1.8 V versus Ag/AgCl to titanium coupons increased the surrounding media pH to approximately 12. An 8-hour exposure to these conditions killed all planktonic bacteria and completely prevented bacterial attachment onto titanium in experiments where sterile titanium coupons were stimulated upon immersion in fresh MRSA bacterial cultures [100]. In contrast, the same study also showed that application of − 1.5 V versus Ag/AgCl for 8 h only increased the pH to around 8 and had no antimicrobial effects [100]. In more recent reports, Canty et al. [69] showed that stimulating titanium coupons with established MRSA biofilms at − 1.8 V versus Ag/AgCl for 24 h increased the media pH to 12 and completely eradicated the biofilm-associated and planktonic MRSA. Whereas stimulation at − 1.5 V versus Ag/AgCl for 24 h increased media pH to 9 and significantly reduced the biofilm-associated CFU by approximately 1-log. However, these authors also determined that alkaline media produced by chemical titration with sodium hydroxide does not have the same bactericidal effects as does alkaline media generated by electrochemical reduction processes [69]. These discrepancies highlight that other mechanisms associated with the electrochemical processes of stimulation are also likely contributing to the antimicrobial outcomes.

The electrochemical generation of hydrogen peroxide by the cathodic reduction reactions has also been suggested as a possible mechanism for the antimicrobial faradaic effects. For example, Lui et al. [79] reported that hydrogen peroxide is produced at the cathode by a low amperage (10–100 µA) electric current and contributes to the bactericidal activity of the stimulation. Babauta et al. [112] also reported hydrogen peroxide accumulation near oxygen-producing biofilms colonized on polarized cathodes. Sultana et al. [92] has shown that application of − 600 mV versus Ag/AgCl to a carbon scaffold for 24 h resulted in the local generation of hydrogen peroxide and produced a 4-log reduction in viable *A. baumannii*. Further, Sultana et al. [93] electrochemically generated a constant concentration of hydrogen peroxide and showed it enhanced efficacy of tobramycin against *P. aeruginosa* biofilms and persister cells.

Hydrogen gas can be generated at the cathode when the applied potential is sufficiently cathodic to promote the water reduction reaction. Several authors [69, 71, 87, 89] have suggested that the evolution and release of hydrogen bubbles at the cathode surface may act to mechanically disrupt the attachment of bacterial biofilms on the electrode and therefore contribute to the antimicrobial processes at the cathode.

3.3.2 Bioelectric effect

The bioelectric effect, first reported by Blenkinsopp et al. [68], refers the synergistic antimicrobial effects when electrical stimulation is combined with antibiotics or biocides. Since this initial report, a large number of subsequent studies have shown the bioelectric effect is active against many clinically relevant bacteria when treated with a variety of electrical stimulation modalities in combination with antibiotics and other disinfectants [68–70, 73, 77, 81–84, 93, 96–98, 105, 113]. This body of literature has been extensively reviewed by Del Pozo et al. [107] and by Freebairn et al. [108]. While the exact mechanism of the bioelectric effect

has not been precisely defined, many potential mechanisms have been proposed including enhanced transport of antimicrobials through the biofilm matrix by electrophoresis [68, 70, 73, 114], enhanced antimicrobial uptake via electroporation [68], better antibiotic penetration due to increased permeability of bacterial membranes induced by electrochemically generated hydrogen peroxide [93], increased cellular metabolism and antimicrobial activity due to electrolytic generation of oxygen [97, 105, 114], altered expression of genes related to antibiotic resistance and transport of small molecules [82], or the combination/interaction of faradaic antimicrobial effects (i.e. pH, hydrogen peroxide) with the antibiotics [69, 70].

One of the difficulties with identifying the mechanism of the bioelectric effect is that many of these studies have been performed with diverse experimental protocols utilizing different combinations of bacteria, antibiotics, chamber designs, electrode materials, stimulation modalities, stimulation magnitudes and durations, and test endpoints. Furthermore, within the context of this present review, only a few studies that report a bioelectric effect have direct relevance to the application of delivering electrical stimulation directly to an orthopedic implant that would function as an isolated electrode (cathode). The previously described in vivo studies by Nodzo et al. [83, 84] showed the combination of CVCES at − 1.8 V versus Ag/AgCl with vancomycin therapy had greater antimicrobial effects than either one of the treatments alone. In addition, Canty et al. [69] has shown that applying CVCES at − 1.5 V versus Ag/AgCl to titanium with concurrent antibiotic therapy provides synergistic reductions in the amount of MRSA and *P. aeruginosa* bacteria that attached to the titanium surface. Furthermore, these authors also reported that the same combination therapy also synergistically reduced the MRSA and *P. aeruginosa* bacterial burden associated with biofilms that were preformed on the titanium surface. It is important to emphasize that this synergy was observed when the MIC of the antibiotics were used. In previous reports of the bioelectric effect it was often necessary to use antibiotic concentrations that were well above the MIC (5-fold to 20-fold greater) to show synergy between electrical stimulation and antibiotics [73, 93, 98, 114]. These results for combining CVCES with antibiotics are encouraging and indicate that future studies are warranted to further evaluate this combined treatment against a broad range of clinically relevant organism.

3.4 Future directions

While there has been substantial research showing that electrical stimulation is associated with broad-spectrum antimicrobial outcomes, the exact mechanism of action governing these antimicrobial effects has not been identified. Amongst others, H_2 gas, pH, electrostatic repulsion, and the bioelectric effect have all been suggested as possible contributors to the antimicrobial outcomes. Future studies should focus on identifying the electrochemical and biological mechanism of action that can subsequently be used to develop targeted and optimized electrical stimulation treatment parameters. Additionally, future in vivo studies regarding the electrochemical control of infection are required to more accurately determine the effects in a living system. Animal studies should assess, in detail, the safety and efficacy of electrical stimulation to determine the optimal treatment parameters. Proper histological assessment following treatments will further enhance the current understanding of the effects electrical stimulation has on surrounding bone and tissue.

4 Electrochemical concepts for sensing of osseointegration and infection

Electrochemical techniques have been utilized as medical diagnostic tools, however most applications are generally focused on assessing the condition of nerve and muscle tissue, not for monitoring the status of an implanted device [115]. One promising technique that could be used to evaluate the implant/tissue interface is electrochemical impedance spectroscopy (EIS) [116]. This technique utilizes the application of a sinusoidal voltage or current oscillation over a range of frequencies and a subsequent analysis of the current or voltage response to determine the impedance characteristics of the electrode. The impedance spectrum can then be fit to equivalent electrical circuit models typically consisting of resistors, capacitors, constant phase elements, inductors and Warburg diffusion elements to represent physical processes at the electrode/environment interface.

Figure 1 illustrates the various EIS experimental setups. Depending on how the EIS measurement is configured, different results can be achieved. For the setup in Fig. 1a, a sinusoidal voltage is applied to the working electrode (WE) and the resulting current response of the counter electrode (CE) is analyzed. This two-electrode method yields information about the interface of both electrodes in the system. In order to study the processes at a single electrode, a reference electrode must be added as in Fig. 1b. The reference electrode establishes a set potential over which there is no current flow, which allows the impedance characteristics of only the working electrode to be analyzed. Figure 1c displays a four-electrode setup for EIS. In this method, a fourth electrode is added called the working sense electrode, which also only measures voltage. A sinusoidal current perturbation is applied between the working and counter electrode, and the resulting voltage between WSE and RE is analyzed. The type of information sought is what determines how the electrodes will be arranged for a given application. Work

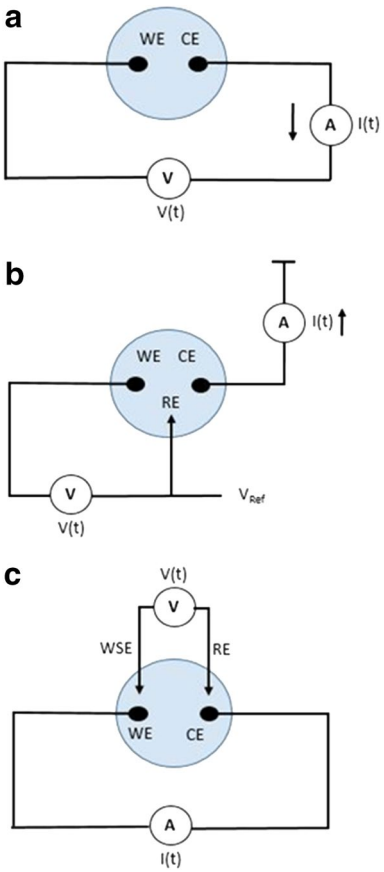

Fig. 1 Two electrode **a** three electrode **b** and four electrode configuration for EIS measurements. Working electrode (WE) counter electrode (CE) reference electrode (RE) and working sense electrode (WSE)

has been done to develop this technique to build models for a variety of tissues including skin, bone, muscle and nerve tissue [117–122]. EIS is also being developed as a method for tracking biofilm formation and assessing the infection status in a clinical setting.

4.1 Electrochemical impedance for assessing bone quality (summary provided in Table 5)

Using in vivo and ex vivo models, EIS has been utilized by several researchers to study the characteristics of bone with [123, 124]. One common application of this method is for the characterization of bone tissue impedance in order to properly position nerve stimulating electrodes [117, 125, 126]. Schaur et al. [117] demonstrated that the thickness and quality of the bone impacted the impedance measured between two electrodes in an ex vivo calf femur model. This study showed a quantifiable difference in impedance based on the presence of soft tissue, trabecular, and cortical bone between the two electrodes, with denser tissue resulting in higher impedance [117]. Work by Teichmann et al. [125] showed that differences in bone layers during craniotomy can be determined using impedance measurements on bipolar electrodes attached to cutting instruments. Balmer et al. [126] studied the impedance characteristics of mastoid bone in an in vivo sheep model. In this work, a custom probe containing two ring electrodes composed of 304 stainless steel was placed into holes drilled into the mastoid bone of sheep. It was found that the resistivity of the bone was linearly dependent on the distance between the electrodes, and the density of the local bone [126].

EIS has also been utilized to assess the bone healing process for both nonunion fractures as well as critical size defects. Collins et al. [127] studied the effects of cathodic electrical stimulation of a titanium wire cathode on both the new bone formation, and the electrical impedance of the titanium cathode in a canine model of nonunion fracture. Their hypothesis was that the impedance of the electrode would increase with the presence of new bone formation. Although this study did show increased bone growth as a function of the applied current, the impedance of the titanium electrode did not significantly increase as a function of bone growth. This was attributed to the formation of a nonosseous tissue directly around the cathode [127]. Gupta et al. [128] developed a method for assessing fracture healing using impedance measurements of external fixation pins that were insulated to only yield signal from the bone tissue. This work was carried out in 14 patients being treated for compound fracture of the tibia. It was shown that the mean difference in impedance increased over an 8 week time course, with a sharp increase in impedance corresponding to fracture union [128]. Lin et al. [129] developed smart bone plates that utilize impedance measurements at gold and platinum microelectrodes inserted into bone defects in a mouse model. This study used both an external fixation model and a titanium bone plate model to assess fracture healing. It was found that the resistance and the reactance increase rapidly in cases where healing occurred properly, and more slowly in poorly healing mice. This increase in impedance was attributed to the transition from blood contact, to cartilage to mineralized bone at the sensor interface. The EIS measurements were compared to X-ray, histology, and μCT results and were found to support the EIS diagnosis of either union or nonunion. This work provides the first example of microscale implanted EIS sensors being used for fracture monitoring [129]. Kozhevnikov et al. [130] monitored the healing of critical size bone defects in rabbits treated with bone scaffolds using two-electrode EIS. In this work, a critical size bone defect was created in rabbit forelimb model, and treated with a scaffold material, or left empty as a control. EIS of the defect site was recorded over a 12-week healing period. The impedance measurements were normalized to healthy bone, and it was found that the scaffold treated mice had significantly higher impedance at

Table 5 A summary of the studies relevant to the evaluation of electrochemical impedance spectroscopy for assessment of bone quality, osseointegration, and infection

Assessment	References	Experimental system	Electrode configuration	Material	Duration	Primary result
Bone quality	Schaur et al. [117]	Ex vivo calf femur	2 electrode	Not specified	N/A	Position dependent change in impedance based on tissue type
	Teichmann et al. [125]	Ex vivo calf femur	2 electrode	Gold	N/A	Detect differences in bone quality during craniotomy
	Balmer et al. [126]	In vivo sheep model	2 electrode	304 stainless steel	In situ	Distance and bone quality between electrodes effects impedance measurement
	Collins et al. [127]	In vivo canine model	3 electrode	Titanium cathode	12 weeks	Cathodic stimulation did not increase impedance around the cathode
	Gupta et al. [128]	In vivo human trial	2 electrode	Steel ex fix pins	8 weeks	Mean increase in impedance increase with healing time, sharp increase with union
	Lin et al. [129]	In vivo mouse model	2 electrode	Gold and platinum interdigitated electrode array	0–28 days and 0–26 days	Measure time course of nonunion fracture healing with implantable microdevice
	Kozhevnikov et al. [130]	In vivo rabbit model	2 electrode	Ag/AgCl	12 weeks	EIS monitored the healing of bone CSD over 12 weeks with bone scaffold treatment
Osseointegration	Clemente et al. [124]	Human in vivo trial	3 electrode	Titanium (working electrode), silver (reference electrode)	90 days	Osseointegration corresponds to an increase in impedance, while clinical complications can cause a decrease in impedance during the healing process
	Fox et al. [131]	In vivo baboon tibia model	3 electrode	Titanium (working electrode), silver (reference electrode)	1 h	No short term changes in impedance during implantation
	Cosoli et al. [132]	In vivo human dental implant	2 electrode	Titanium implant, stainless steel electrode	In situ	Determine difference between healthy, inflamed, and infected dental implants with EIS
	Duan et al. [133]	In vivo cat model	2 electrode	Platinum band electrode	60 days	Impedance increase with 6 month implantation time
	Arpaia et al. [134]	Ex vivo cow femur	2 electrode	Titanium screw electrodes	N/A	Number of screw cycles decreased bone/electrode contact, which decreased impedance

Table 5 (continued)

Assessment	References	Experimental system	Electrode configuration	Material	Duration	Primary result
Infection	Farrow et al. [138]	In vitro simulated wound fluid	2 electrode	Ag/AgCl	16 h	Impedance normalization is a useful technique for monitoring bacterial attachment
	Ward et al. [136]	In vitro simulated wound fluid	2 electrode	Screen printed carbon	24 h	Normalized phase angle can determine presence of *P. aeruginosa*, and distinguish between mucoid and non-mucoid strains
	Kim et al. [140]	In vitro simulated wound fluid	2 electrode	Gold interdigitated electrode array	1 h	Bacterial attachment decreased capacitance in interdigitated electrode array; single frequency can be used in real time
	Paredes et al. [141]	96 well plate	2 electrode	Gold interdigitated electrode array	24 h	Biofilm formation causes 35% increase in resistance after a few hours
	Paredes et al. [142]	In vitro venous catheter phantom	2 electrode	Gold interdigitated electrode array	48 h	55% maximum change in impedance parameters after 10 h
	Hoyos-Nogués et al. [146]	In vitro	2 electrode	Antimicrobial peptide functionalized interdigitated electrode array	5 h	Linear increase in resistance to *S. sanguinis* in artificial saliva
	Ahmed et al. [147]	In vitro	2 electrode	Antibody functionalized gold interdigitated electrode array	30 min	Sensitive detection of *S. pyogenes*

the defect site than the control animals at all time points. This suggests that EIS can also be applied as a method for tracking the treatment of critical size bone defects [130].

4.2 Electrochemical impedance for assessing osseointegration (summary provided in Table 5)

The previously discussed works have demonstrated that EIS can be applied to assess local bone quality. However, for EIS to be adapted as a method for quantifying osseointegration, the impedance properties of the intended implant must be shown to change characteristically with osseointegration status. An early study by Fox et al. [131] utilized a titanium cancellous access port with an electrochemical transducer to study the short term impedance behavior of a titanium electrode in a baboon tibia model. This work showed only small changes in the impedance characteristics of the implant when measured over 1 h of implantation. Other work utilized two-electrode EIS to evaluate inflammation surrounding dental implants in vivo [132]. In this study, the impedance was assessed between the titanium implant and a smaller steel electrode attached to different points on the gingiva in an attempt to localize the site of inflammation. EIS was measured on implants with healthy tissue, inflammation, and peri-implantitis. A linear combination of a resistor and a capacitor were used to model the data, and the resistance was determined to be the most relevant parameter to track inflammation. It was found that the implants with inflammation had a 35% decrease in impedance modulus, which was attributed to hyperaemia in the surrounding tissue. Peri-implantitis decreased the impedance modulus by 56%, which was attributed to loss of bone surrounding the implant [132]. EIS has also been applied to assess cochlear implants. Duan et al. [133] conducted a study to investigate the tissue/electrode interface inside the cochlea of a cat using platinum band electrode. These investigators found that the impedance at the tissue/electrode interface increased during a 6-month implantation period, and attributed this to changes in local extracellular fluid composition related to inflammation and encapsulation of the electrodes [133].

The utilization of EIS to measure the osseointegration of metallic prosthesis has been studied in detail by Clemente and Arpaia [134]. This group developed a custom microcontroller based platform capable of measuring EIS on metallic prosthetics in ex vivo and in vivo models [134]. Using an ex vivo cow femur model, it was shown that EIS could be used to track changes in implant/tissue contact. To accomplish this, dental implants were screwed into and out of the femur for up to 4 cycles to simulate different bone/implant contact. The impedance spectrum was found to change as a function of the bone/implant contact [134]. For in vivo testing, the titanium fixture of BAHA® cochlear implants implanted into 10 patients were analyzed [124]. This work utilized a three-electrode setup, with the titanium fixture being the working electrode and two Ag/AgCl skin electrodes completing the system. Measurements for this study were conducted at 1, 7, 30 and 90 days post implantation. During a normal osseointegration, there was a large increase in impedance between day 7 and 30. For a case with a clinical complication of seroma, the impedance of the implant decreased sharply between day 30 and day 90, corresponding to a decrease in bone contact at the implant [124]. Taken together, these studies suggest that tracking the impedance characteristics of titanium implants could be a useful and noninvasive method for determining osseointegration.

4.3 Electrochemical impedance sensing of infection (summary provided in Table 5)

One of the biggest challenges facing OI prosthesis implementation is the risk of infection at both the bone and the percutaneous site. In addition to being notoriously difficult to treat, implant associated infections are particularly difficult to detect at the early stages of infection [135]. Electrochemical detection of infection and biofilms is being pursued to help address this issue [136]. There are three primary methods by which EIS is used to detect bacteria. The first method is single frequency impedance measurements over time. This setup, also called "impedance microbiology", utilizes two planar electrodes and measures the solution impedance between the electrodes. The change in media conductivity is used to assess the presence of bacteria in solution. This method was found to be useful in the point of care detection in medical contexts [137]. Another method for bacteria detection is impedance-splitting, where the impedance is measured at two different frequencies, one in the < 100 Hz range to measure the electrode interface impedance and another in the 10 kHz range to assess the solution resistance. This method is commonly applied in the detection of foodborne pathogens [137]. Utilizing full spectrum EIS measurements can also be applied for microorganism detection. This approach was used by Farrow et al. [138] to detect *S. aureus* in simulated wound fluid conditions. In this work, the impedance parameters were normalized to an initial measured impedance value, and the change in this normalized impedance was used to track bacterial growth in real time. The intended application of this work was to develop a method for tracking bacterial growth under wound dressings using a two Ag/AgCl electrode configuration. It was also shown by Ward et al. [136] that that same impedance normalization technique could be used to determine the presence of *P. aeruginosa* on screen printed carbon electrodes by differences in the phase angle measurements. Additionally, this method was found to be able to distinguish between mucoid and non-mucoid forms of *P. aeruginosa* [136].

Interdigitated electrode arrays (IDAs) are a newer electrode configuration in which EIS is being widely applied for the detection of microorganisms. IDAs offer a more idealized sensing platform than bulk and planar electrodes to improve the sensitivity of bacterial detection [139]. Kim et al. [140] used an interdigitated gold IDA to rapidly detect the presence of *P. aeruginosa*. This work found that the presence of the bacteria resulted in a decrease in the calculated capacitance compared to the control with no bacteria. It was also found that the capacitance at a fixed frequency of 100 Hz decreased with the presence of *P. aeruginosa*, which suggests that single frequency impedance measurements can also be used with IDAs. Paredes et al. also utilized gold IDAs in a 96 well plate configuration to monitor *S. aureus* and *S. epidermidis* biofilm formation in real time. In this system, the calculated resistance of the electrodes was determined to increase by up to 35% within a few hours of inoculation, which was taken to correspond to bacterial attachment and biofilm formation [141]. This IDA was then further utilized as the sensing element in a smart central venous catheter device [142]. In vitro tests of this device showed that it was able to detect the formation of an *S. epidermidis* biofilm within a catheter port in real time. It was shown that both the measured resistance and capacitance were influenced by the biofilm formation on the sensor according to a previously developed model [143].

Microelectrodes and electrode arrays can also be functionalized with a variety of biorecognition elements that can allow for the specific detection of bacteria in complex media, such as in the body or from body fluids. Biorecognition elements that have been used to detect bacteria include antibodies, enzymes, aptamers, peptides, and bacteriophages [144]. The working principle of impedimetric biosensors is that the specific binding of the target molecule will cause a quantifiable change in impedance characteristics of the transducer electrode. This allows for the selectivity of the electrode to be increased significantly compared to bare electrode surfaces [145]. Hoyos-Nogués et al. [146] developed an antimicrobial peptide based impedimetric sensor for the sensitive detection of the periodontal pathogen *Streptococcus sanguinis*. This IDA sensor had a linear increase in the solution resistance parameter as a function of the log CFU in the test solutions of KCl and artificial saliva [146]. Ahmed et al. [147] studied an impedimetric immunosensor for the specific detection of the pathogen *Streptococcus pyogenes (S. pyogenes).* In this work, gold electrodes were functionalized with *S. pyogenes* antibodies as a biorecognition element. The percentage change in charge transfer resistance of the electrode was found to be linear when exposed to solutions containing *S. pyogenes* from 10^4 to 10^7 cells/mL [147]. Although functionalized biosensors can improve the sensitivity and selectivity of impedimetric sensors, they can suffer from problems with degradation of the biorecognition element [145].

4.4 Future directions

The majority of impedemetric sensors that are being developed are intended to be point of care diagnostic measures, rather than in vivo detection methods. However, in some cases electrochemical sensors arrays and devices are being developed to detect infection in specific locations of the body, including blood, skin wounds and venous catheters [142, 148, 149]. This approach would be difficult to adopt for OI implant applications in part due to the large size of the implant. A sensor array would have to be located close enough to the site of the infection, or it would have to cover a considerable amount of the implant surface. This could cause issues with the osseointegration of the implant, as this relies heavily on the surface properties of titanium/titanium alloys. The literature reviewed in the previous sections shows that there is evidence to support that EIS based methods are capable of detecting both osseointegration and infection separately. However, the use of EIS to monitor the osseointegration status of OI orthopedic prosthetics has yet to be rigorously investigated. Additionally, infection can be considered a clinical complication following OI implant placement. If the presence of infection were to cause a deficit in the osseointegration of the implant, it may be able to be detected with EIS at the early stages of infection. This could provide a rapid and noninvasive method for assessing the osseointegration and infection status of OI implants.

5 Conclusion

As shown in this review, electrochemical methods have great potential for both sensing and enhancing the osseointegration and infection control of orthopedic implants. Current and voltage-controlled DC stimulations have been shown to be effective at eliminating bacterial biofilms on, and in proximity to, stimulating electrodes. In the presence of clinically relevant disinfectants, these effects have been enhanced, creating a synergistic antimicrobial reduction. Therefore, utilizing the metallic implant to deliver localized electrical stimulation may be a clinically advantageous method for preventing and/or treating recalcitrant implant-associated infections that are a prominent source of patient morbidity and increased healthcare costs. In addition to the antimicrobial benefits, cathodic stimulation has shown beneficial influence on bone tissue. While DC electrical stimulation is used clinically for enhancing fracture healing and bone fusions, it has not yet been utilized clinically for enhancing osseointegration of titanium implants. One of the remaining challenges is to identify the optimal electrical stimulation parameters that

have greatest beneficial influence on osseointegration and that have maximal antimicrobial effects. Once these optimal stimulation parameters are known, electrochemical methods could be used to both control infection, as well as promote osseointegration. Another clinical challenge is the accurate and timely diagnosis of implant loosening and infection. As shown in this review, EIS is a diagnostic technique that holds promise for assessing these orthopedic implant complications. As such, additional studies are warranted to rigorously evaluate the use of EIS to monitor the osseointegration and infection status of an orthopedic implant. Ideally, an electrochemically-based, closed-loop system will be developed which utilizes the orthopedic implant as an electrode that can both monitor implant performance criteria and respond when needed with an optimal electrical stimulus to enhance osseointegration and mitigate infections. The development of such a system would have great utility for a wide range of orthopedic implants including osseointegrated prosthetic limbs, total joint prostheses, fracture hardware, mega-prostheses and may also provide solutions for dental peri-implantitis.

Acknowledgements MTE has received research grants from the Office of Naval Research, Garwood Medical Devices, Zimmer Biomet, Depuy Synthes, and Lima Corporate.

Funding Office of Naval Research Grant: N00014-16-1-3187 (MTE).

Compliance with ethical standards

Conflict of interest The authors declare that they have no conflict of interest.

Ethical approval The authors did not perform any studies with human participants or animals to write this review article.

References

1. Thesleff A, Brånemark R, Håkansson B, Ortiz-Catalan M. Biomechanical characterisation of bone-anchored implant systems for amputation limb prostheses: a systematic review. Ann Biomed Eng. 2018;46(3):377–91.
2. Williams E, Rydevik B, Johns R, Brånemark P-I, editors. Osseoperception and musculo-skeletal function. Tranemo: Tranemo Typo; 1999.
3. Bard AJ, Faulkner LR. Electrochemcial methods: fundamentals and applications. 2nd ed. New York: Wiley; 2000.
4. Bassett CA, Becker RO. Generation of electric potentials by bone in response to mechanical stress. Science. 1962;137:1063–4.
5. Fukada E, Yasuda I. On piezoelectric effect of bone. J Phys Soc Jpn. 1957;12:1158–62.
6. Yasuda I, Noguchi K, Sata T. Dynamic callus and electrical callus. J Bone Jt Surg. 1955;73A:1292–3.
7. Friedenberg ZB, Andrews ET, Smolenski BI, Pearl BW, Brighton CT. Bone reaction to varying amounts of direct current. Surg Gynecol Obstet. 1970;131(5):894–9.
8. Friedenberg ZB, Roberts PG Jr, Didizian NH, Brighton CT. Stimulation of fracture healing by direct current in the rabbit fibula. J Bone Jt Surg Am. 1971;53(7):1400–8.
9. Friedenberg ZB, Zemsky LM, Pollis RP, Brighton CT. The response of non-traumatized bone to direct current. J Bone Jt Surg Am. 1974;56(5):1023–30.
10. Brighton CT, Adler S, Black J, Itada N, Friedenberg ZB. Cathodic oxygen consumption and electrically induced osteogenesis. Clin Orthop Relat Res. 1975;107:277–82.
11. Brighton CT, Friedenberg ZB. Electrical stimulation and oxygen tension. Ann N Y Acad Sci. 1974;238:314–20.
12. Spadaro JA, Becker RO. Function of implanted cathodes in electrode-induced bone growth. Med Biol Eng Comput. 1979;17(6):769–75.
13. Baranowski JTJ, Black J, Brighton CT. Microenvironmental changes associated with electrical stimulation of osteogenesis by direct current. In: Transactions of the bioelectrical repair and growth society. 1982. p. 47.
14. Baranowski JTJ. Electrical stimulation of osteogenesis by direct current: electrochemically mediated microenvironmental alterations. Philadelphia: University of Pennsylvania; 1983.
15. Baranowski TJ, Black J. The mechanism of faradaic stimulation of osteogenesis. In: Blank M, Findle E, editors. Mechanistic approaches to interactions of electrical and electromagnetic fields with living systems. New York: Plenum Publishing Co.; 1987. p. 399–416.
16. Tuncay OC, Ho D, Barker MK. Oxygen tension regulates osteoblast function. Am J Orthod Dentofac Orthop. 1994;105(5):457–63.
17. Bushinsky DA. Metabolic alkalosis decreases bone calcium efflux by suppressing osteoclasts and stimulating osteoblasts. Am J Physiol. 1996;271(1 Pt 2):F216–22.
18. Kaysinger KK, Ramp WK. Extracellular pH modulates the activity of cultured human osteoblasts. J Cell Biochem. 1998;68(1):83–9.
19. Cho M, Hunt TK, Hussain MZ. Hydrogen peroxide stimulates macrophage vascular endothelial growth factor release. Am J Physiol Heart Circ Physiol. 2001;280(5):H2357–63.
20. Brighton CT, Friedenberg ZB, Black J, Esterhai JL Jr, Mitchell JE, Montique F Jr. Electrically induced osteogenesis: relationship between charge, current density, and the amount of bone formed: introduction of a new cathode concept. Clin Orthop Relat Res. 1981;161:122–32.
21. Baranowski TJJ, Black J. The role of cathodic potential in electrical stimulation of osteogenesis by direct current. Trans Orthop Res Soc. 1983;8:352.
22. Campbell CE, Higginbotham DV, Baranowski TJ. A constant cathodic potential device for faradic stimulation of osteogenesis. Med Eng Phys. 1995;17(5):337–46.
23. Dymecki SM, Black J, Brighton CT. The cathodic potential dose-response relationship for medullary osteogenesis with stainless steel electrodes. Trans Bioelectr Repair Growth Soc. 1984;4:29.
24. Griffin M, Bayat A. Electrical stimulation in bone healing: critical analysis by evaluating levels of evidence. Eplasty. 2011;11:e34.
25. Branemark P-I. Osseointegration and its experimental background. J Prosthet Dent. 1983;50(3):399–410.
26. Branemark R, Branemark PI, Rydevik B, Myers RR. Osseointegration in skeletal reconstruction and rehabilitation: a review. J Rehabil Res Dev. 2001;38(2):175–81.
27. Shah FA, Thomsen P, Palmquist A. Osseointegration and current interpretations of the bone-implant interface. Acta Biomater. 2019;84:1–15.
28. Shah FA, Stenlund P, Martinelli A, Thomsen P, Palmquist A. Direct communication between osteocytes and acid-etched titanium implants with a sub-micron topography. J Mater Sci Mater Med. 2016;27(11):167.

29. Shah FA, Wang X, Thomsen P, Grandfield K, Palmquist A. High-resolution visualization of the osteocyte lacuno-canalicular network juxtaposed to the surface of nanotextured titanium implants in human. ACS Biomater Sci Eng. 2015;1(5):305–13.
30. Albrektsson T, Brånemark P-I, Hansson H-A, Kasemo B, Larsson K, Lundström I, McQueen DH, Skalak R. The interface zone of inorganic implantsIn vivo: titanium implants in bone. J Ann Biomed Eng. 1983;11(1):1–27.
31. Binkley DM, Grandfield K. Advances in multiscale characterization techniques of bone and biomaterials interfaces. ACS Biomater Sci Eng. 2018;4(11):3678–90.
32. Grandfield K, Gustafsson S, Palmquist A. Where bone meets implant: the characterization of nano-osseointegration. Nanoscale. 2013;5(10):4302–8.
33. Wang X, Shah FA, Palmquist A, Grandfield K. 3D characterization of human nano-osseointegration by on-axis electron tomography without the missing wedge. ACS Biomater Sci Eng. 2017;3(1):49–55.
34. Bearinger JP, Orme CA, Gilbert JL. Direct observation of hydration of TiO2 on Ti using electrochemical AFM: freely corroding versus potentiostatically held. Surf Sci. 2001;491(3):370–87.
35. Bearinger JP, Orme CA, Gilbert JL. In situ imaging and impedance measurements of titanium surfaces using AFM and SPIS. Biomaterials. 2003;24(11):1837–52.
36. Bearinger JP, Orme CA, Gilbert JL. Effect of hydrogen peroxide on titanium surfaces: in situ imaging and step-polarization impedance spectroscopy of commercially pure titanium and titanium, 6-aluminum, 4-vanadium. J Biomed Mater Res Part A. 2003;67A(3):702–12.
37. Brooks E, Tobias M, Krautsak K, Ehrensberger M. The influence of cathodic polarization and simulated inflammation on titanium electrochemistry. J Biomed Mater Res B Appl Biomater. 2014;102(7):1445–53.
38. Ciolko AA, Tobias M, Ehrensberger MT. The effect of fretting associated periodic cathodic potential shifts on the electrochemistry and in vitro biocompatibility of commercially pure titanium. J Biomed Mater Res Part B. 2016;104(8):1591-1601.
39. Ehrensberger MT, Gilbert JL. The effect of scanning electrochemical potential on the short-term impedance of commercially pure titanium in simulated biological conditions. J Biomed Mater Res Part A. 2010;94A(3):781–9.
40. Ehrensberger MT, Gilbert JL. The effect of static applied potential on the 24-hour impedance behavior of commercially pure titanium in simulated biological conditions. J Biomed Mater Res B Appl Biomater. 2010;93B(1):106–12.
41. Ehrensberger MT, Sivan S, Gilbert JL. Titanium is not "the most biocompatible metal" under cathodic potential: the relationship between voltage and MC3T3 preosteoblast behavior on electrically polarized cpTi surfaces. J Biomed Mater Res Part A. 2010;93(4):1500.
42. Pan J, Liao H, Leygraf C, Thierry D, Li J. Variation of oxide films on titanium induced by osteoblast-like cell culture and the influence of an H2O2 pretreatment. J Biomed Mater Res. 1998;40(2):244–56.
43. Tengvall P, Lundström I, Sjöqvist L, Elwing H, Bjursten LM. Titanium-hydrogen peroxide interaction: model studies of the influence of the inflammatory response on titanium implants. Biomaterials. 1989;10(3):166.
44. Spriano S, Yamaguchi S, Baino F, Ferraris S. A critical review of multifunctional titanium surfaces: new frontiers for improving osseointegration and host response, avoiding bacteria contamination. Acta Biomater. 2018;79:1–22.
45. Pound BG. Passive films on metallic biomaterials under simulated physiological conditions. J Biomed Mater Res Part A. 2014;102(5):1595–604.
46. Bodamyali T, Kanczler JM, Simon B, Blake DR, Stevens CR. Effect of faradic products on direct current-stimulated calvarial organ culture calcium levels. Biochem Biophys Res Commun. 1999;264(3):657–61.
47. Dauben TJ, Ziebart J, Bender T, Zaatreh S, Kreikemeyer B, Bader R. A novel in vitro system for comparative analyses of bone cells and bacteria under electrical stimulation. Biomed Res Int. 2016;2016:5178640.
48. Ercan B, Webster TJ. Greater osteoblast proliferation on anodized nanotubular titanium upon electrical stimulation. Int J Nanomed. 2008;3(4):477–85.
49. Ercan B, Webster TJ. The effect of biphasic electrical stimulation on osteoblast function at anodized nanotubular titanium surfaces. Biomaterials. 2010;31(13):3684–93.
50. Qiu Q, Sayer M, Shen X, Davies JE. A system designed for the study of cell activity under electrical stimulation. J Biotechnol Tech. 1995;9(3):209–14.
51. Wang Q, Zhong S, Ouyang J, Jiang L, Zhang Z, Xie Y, Luo S. Osteogenesis of electrically stimulated bone cells mediated in part by calcium ions. Clin Orthop Relat Res. 1998;348:259–68.
52. Wang Q, Zhong S, Xie Y, Zhang Z, Yang G. Electrochemical reactions during constant DC current stimulation: an in vitro experiment with cultured rat calvarial cells. Electro Magnetobiol. 1995;14(1):31–40.
53. Gilbert JL, Zarka L, Chang E, Thomas CH. The reduction half cell in biomaterials corrosion: oxygen diffusion profiles near and cell response to polarized titanium surfaces. J Biomed Mater Res. 1998;42(2):321–30.
54. Gittens RA, Olivares-Navarrete R, Rettew R, Butera RJ, Alamgir FM, Boyan BD, Schwartz Z. Electrical polarization of titanium surfaces for the enhancement of osteoblast differentiation. Bioelectromagnetics. 2013;34(8):599–612.
55. Haeri M, Wöllert T, Langford GM, Gilbert JL. Voltage-controlled cellular viability of preosteoblasts on polarized cpTi with varying surface oxide thickness. Bioelectrochemistry. 2013;94:53–60.
56. Kalbacova M, Roessler S, Hempel U, Tsaryk R, Peters K, Scharnweber D, Kirkpatrick JC, Dieter P. The effect of electrochemically simulated titanium cathodic corrosion products on ROS production and metabolic activity of osteoblasts and monocytes/macrophages. Biomaterials. 2007;28(22):3263–72.
57. Sivan S, Kaul S, Gilbert JL. The effect of cathodic electrochemical potential of Ti–6Al–4V on cell viability: voltage threshold and time dependence. J Biomed Mater Res B Appl Biomater. 2013;101(8):1489–97.
58. Bins-Ely LM, Cordero EB, Souza JCM, Teughels W, Benfatti CAM, Magini RS. In vivo electrical application on titanium implants stimulating bone formation. J Periodontal Res. 2017;52(3):479–84.
59. Colella SM, Miller AG, Stang RG, Stoebe TG, Spengler DM. Fixation of porous titanium implants in cortical bone enhanced by electrical stimulation. J Biomed Mater Res. 1981;15(1):37–46.
60. Shayesteh YS, Eslami B, Dehghan MM, Vaziri H, Alikhassi M, Mangoli A, Khojasteh A. The effect of a constant electrical field on osseointegration after immediate implantation in dog mandibles: a preliminary study. J Prosthodont. 2007;16(5):337–42.
61. Song JK, Cho TH, Pan H, Song YM, Kim IS, Lee TH, Hwang SJ, Kim SJ. An electronic device for accelerating bone formation in tissues surrounding a dental implant. Bioelectromagnetics. 2009;30(5):374–84.
62. Dergin G, Akta M, Gursoy B, Devecioglu Y, Kurkcu M, Benlidayi E. Direct current electric stimulation in implant osseointegration: an experimental animal study with sheep. J Oral Implantol. 2013;39(6):671–9.
63. Isaacson BM, Brunker LB, Brown AA, Beck JP, Burns GL, Bloebaum RD. An evaluation of electrical stimulation for

improving periprosthetic attachment. J Biomed Mater Res B Appl Biomater. 2011;97B(1):190–200.
64. Shafer DM, Rogerson K, Norton L, Bennett J. The effect of electrical perturbation on osseointegration of titanium dental implants: a preliminary study. J Oral Maxillofac Surg. 1995;53(9):1063–8.
65. Ehrensberger MT, Tobias ME, Nodzo SR, Hansen LA, Luke-Marshall NR, Cole RF, Wild LM, Campagnari AA. Cathodic voltage-controlled electrical stimulation of titanium implants as treatment for methicillin-resistant *Staphylococcus aureus* periprosthetic infections. Biomaterials. 2015;41:97–105.
66. Ehrensberger M, Campagnari A, Luke-Marshall N, Gilbert J, Takeuchi E. Electrochemical eradication of microbes on surfaces of objects. US Patent No 9,616,142.
67. Spadaro JA. Mechanical and electrical interactions in bone remodeling. Bioelectromagnetics. 1997;18(3):193–202.
68. Blenkinsopp SA, Khoury AE, Costerton JW. Electrical enhancement of biocide efficacy against Pseudomonas-aeruginosa biofilms. Appl Environ Microbiol. 1992;58(11):3770–3.
69. Canty MK, Hansen LA, Tobias M, Spencer S, Henry T, Luke-Marshall NR, Campagnari AA, Ehrensberger MT. Antibiotics enhance prevention and eradication efficacy of cathodic-voltage-controlled electrical stimulation against titanium-associated methicillin-resistant *Staphylococcus aureus* and *Pseudomonas aeruginosa* biofilms. mSphere. 2019;4(3):e00178-19.
70. Costerton JW, Ellis B, Lam K, Johnson F, Khoury AE. Mechanism of electrical enhancement of efficacy of antibiotics in killing biofilm bacteria. Antimicrob Agents Chemother. 1994;38(12):2803–9.
71. Dargahi M, Hosseinidoust Z, Tufenkji N, Omanovic S. Investigating electrochemical removal of bacterial biofilms from stainless steel substrates. Colloids Surf B. 2014;117:152–7.
72. Del Pozo JL, Rouse MS, Euba G, Kang CI, Mandrekar JN, Steckelberg JM, Patel R. The electricidal effect is active in an experimental model of *Staphylococcus epidermidis* chronic foreign body osteomyelitis. Antimicrob Agents Chemother. 2009;53(10):4064–8.
73. del Pozo JL, Rouse MS, Mandrekar JN, Sampedro MF, Steckelberg JM, Patel R. Effect of electrical current on the activities of antimicrobial agents against *Pseudomonas aeruginosa*, *Staphylococcus aureus*, and *Staphylococcus epidermidis* biofilms. Antimicrob Agents Chemother. 2009;53(1):35–40.
74. del Pozo JL, Rouse MS, Mandrekar JN, Steckelberg JM, Patel R. The electricidal effect: reduction of Staphylococcus and Pseudomonas biofilms by prolonged exposure to low-intensity electrical current. Antimicrob Agents Chemother. 2009;53(1):41–5.
75. Dusane DH, Lochab V, Jones T, Peters CW, Sindeldecker D, Das A, Roy S, Sen CK, Subramaniam VV, Wozniak DJ, Prakash S, Stoodley P. Electroceutical Treatment of Pseudomonas aeruginosa Biofilms. Sci Rep. 2019;9(1):2008.
76. Hong SH, Jeong J, Shim S, Kang H, Kwon S, Ahn KH, Yoon J. Effect of electric currents on bacterial detachment and inactivation. Biotechnol Bioeng. 2008;100(2):379–86.
77. Jass J, LappinScott HM. The efficacy of antibiotics enhanced by electrical currents against *Pseudomonas aeruginosa* biofilms. J Antimicrob Chemother. 1996;38(6):987–1000.
78. Kim YW, Subramanian S, Gerasopoulos K, Ben-Yoav H, Wu H-C, Quan D, Carter K, Meyer MT, Bentley WE, Ghodssi R. Effect of electrical energy on the efficacy of biofilm treatment using the bioelectric effect. Npj Biofilms Microbiomes. 2015;1:15016.
79. Liu WK, Brown MR, Elliott TS. Mechanisms of the bactericidal activity of low amperage electric current (DC). J Antimicrob Chemother. 1997;39(6):687–95.
80. Mohn D, Zehnder M, Stark WJ, Imfeld T. Electrochemical Disinfection of dental implants: a proof of concept. PLoS ONE. 2011;6(1):6.
81. Niepa THR, Gilbert JL, Ren DC. Controlling *Pseudomonas aeruginosa* persister cells by weak electrochemical currents and synergistic effects with tobramycin. Biomaterials. 2012;33(30):7356–65.
82. Niepa THR, Snepenger LM, Wang H, Sivan S, Gilbert JL, Jones MB, Ren D. Sensitizing *Pseudomonas aeruginosa* to antibiotics by electrochemical disruption of membrane functions. Biomaterials. 2016;74:267–79.
83. Nodzo S, Tobias M, Hansen L, Luke-Marshall NR, Cole R, Wild L, Campagnari AA, Ehrensberger MT. Cathodic electrical stimulation combined with vancomycin enhances treatment of methicillin-resistant *Staphylococcus aureus* implant-associated infections. Clin Orthop Relat Res. 2015;473:2856–64.
84. Nodzo SR, Tobias M, Ahn R, Hansen L, Luke-Marshall NR, Howard C, Wild L, Campagnari AA, Ehrensberger MT. Cathodic voltage-controlled electrical stimulation plus prolonged vancomycin reduce bacterial burden of a titanium implant-associated infection in a rodent model. Clin Orthop Relat Res. 2016;474:1668–75.
85. Poortinga AT, Bos R, Busscher HJ. Reversibility of bacterial adhesion at an electrode surface. Langmuir. 2001;17(9):2851–6.
86. Poortinga AT, Smit J, van der Mei HC, Busscher HJ. Electric field induced desorption of bacteria from a conditioning film covered substratum. Biotechnol Bioeng. 2001;76(4):395–9.
87. Rabinovitch C, Stewart PS. Removal and inactivation of *Staphylococcus epidermidis* biofilms by electrolysis. Appl Environ Microbiol. 2006;72(9):6364–6.
88. Sandvik EL, McLeod BR, Parker AE, Stewart PS. Direct electric current treatment under physiologic saline conditions kills *Staphylococcus epidermidis* biofilms via electrolytic generation of hypochlorous acid. PLoS ONE. 2013;8(2):e55118.
89. Schneider S, Rudolph M, Bause V, Terfort A. Electrochemical removal of biofilms from titanium dental implant surfaces. Bioelectrochemistry. 2018;121:84–94.
90. Shirtliff ME, Bargmeyer A, Camper AK. Assessment of the ability of the bioelectric effect to eliminate mixed-species biofilms. Appl Environ Microbiol. 2005;71(10):6379–82.
91. Stoodley P, deBeer D, Lappin-Scott HM. Influence of electric fields and pH on biofilm structure as related to the bioelectric effect. Antimicrob Agents Chemother. 1997;41(9):1876–9.
92. Sultana ST, Atci E, Babauta JT, Mohamed Falghoush A, Snekvik KR, Call DR, Beyenal H. Electrochemical scaffold generates localized, low concentration of hydrogen peroxide that inhibits bacterial pathogens and biofilms. Sci Rep. 2015;5:14908.
93. Sultana ST, Call DR, Beyenal H. Eradication of *Pseudomonas aeruginosa* biofilms and persister cells using an electrochemical scaffold and enhanced antibiotic susceptibility. NPJ Biofilms Microbiomes. 2016;2:2.
94. van der Borden AJ, van der Mei HC, Busscher H. Electric block current induced detachment from surgical stainless steel and decreased viability of Staphylococcus epidermidis. Biomaterials. 2005;26(33):6731–5.
95. van der Borden AJ, van der Werf H, van der Mei HC, Busscher HJ. Electric current-induced detachment of *Staphylococcus epidermidis* biofilms from surgical stainless steel. Appl Environ Microbiol. 2004;70(11):6871–4.
96. Wang H, Ren D. Controlling *Streptococcus mutans* and *Staphylococcus aureus* biofilms with direct current and chlorhexidine. AMB Express. 2017;7(1):204.
97. Wattanakaroon W, Stewart PS. Electrical enhancement of *Streptococcus gordonii* biofilm killing by gentamicin. Arch Oral Biol. 2000;45(2):167–71.

98. Wellman N, Fortun SM, McLeod BR. Bacterial biofilms and the bioelectric effect. Antimicrob Agents Chemother. 1996;40(9):2012–4.
99. Busalmen JP, de Sánchez SR. Adhesion of *Pseudomonas fluorescens* (ATCC 17552) to nonpolarized and polarized thin films of gold. Appl Environ Microbiol. 2001;67(7):3188–94.
100. Canty M, Luke-Marshall N, Campagnari A, Ehrensberger M. Cathodic voltage-controlled electrical stimulation of titanium for prevention of methicillin-resistant *Staphylococcus aureus* and *Acinetobacter baumannii* biofilm infections. Acta Biomater. 2017;48:451–60.
101. Del Pozo JL, Rouse MS, Euba G, Greenwood-Quaintance KE, Mandrekar JN, Steckelberg JM, Patel R. Prevention of *Staphylococcus epidermidis* biofilm formation using electrical current. J Appl Biomater Funct Mater. 2014;12(2):81–3.
102. Shim S, Hong SH, Tak Y, Yoon J. Prevention of *Pseudomonas aeruginosa* adhesion by electric currents. Biofouling. 2011;27(2):217–24.
103. van der Borden AJ, Maathuis PGM, Engels E, Rakhorst G, van der Mei HC, Busscher HJ, Sharma PK. Prevention of pin tract infection in external stainless steel fixator frames using electric current in a goat model. Biomaterials. 2007;28(12):2122–6.
104. Schmidt-Malan SM, Karau MJ, Cede J, Greenwood-Quaintance KE, Brinkman CL, Mandrekar JN, Patel R. Antibiofilm activity of low-amperage continuous and intermittent direct electrical current. Antimicrob Agents Chemother. 2015;59(8):4610.
105. Stewart PS, Wattanakaroon W, Goodrum L, Fortun SM, McLeod BR. Electrolytic generation of oxygen partially explains electrical enhancement of tobramycin efficacy against *Pseudomonas aeruginosa* biofilm. Antimicrob Agents Chemother. 1999;43(2):292–6.
106. van der Borden AJ, van der Mei HC, Busscher HJ. Electric-current-induced detachment of *Staphylococcus epidermidis* strains from surgical stainless steel. J Biomed Mater Res B Appl Biomater. 2004;68(2):160–4.
107. Del Pozo JL, Rouse MS, Patel R. Bioelectric effect and bacterial biofilms: a systematic review. Int J Artif Organs. 2008;31(9):786–95.
108. Freebairn D, Linton D, Harkin-Jones E, Jones DS, Gilmore BF, Gorman SP. Electrical methods of controlling bacterial adhesion and biofilm on device surfaces. Expert Rev Med Devices. 2013;10(1):85–103.
109. Sultana ST, Babauta JT, Beyenal H. Electrochemical biofilm control: a review. Biofouling. 2015;31(9–10):745–58.
110. Poortinga AT, Bos R, Norde W, Busscher HJ. Electric double layer interactions in bacterial adhesion to surfaces. Surf Sci Rep. 2002;47(1):1–32.
111. Sweity A, Ying W, Belfer S, Oron G, Herzberg M. pH effects on the adherence and fouling propensity of extracellular polymeric substances in a membrane bioreactor. J Membr Sci. 2011;378(1–2):186–93.
112. Babauta JT, Nguyen HD, Istanbullu O, Beyenal H. Microscale gradients of oxygen, hydrogen peroxide, and pH in freshwater cathodic biofilms. ChemSusChem. 2013;6(7):1252–61.
113. Pickering SAW, Bayston R, Scammell BE. Electromagnetic augmentation of antibiotic efficacy in infection of orthopaedic implants. J Bone Jt Surg Br. 2003;85B(4):588–93.
114. Jass J, Costerton JW, Lappin-Scott HM. The effect of electrical currents and tobramycin on *Pseudomonas aeruginosa* biofilms. J Ind Microbiol. 1995;15(3):234–42.
115. Sinkjaer T, Haugland M, Inmann A, Hansen M, Nielsen KD. Biopotentials as command and feedback signals in functional electrical stimulation systems. Med Eng Phys. 2003;25(1):29–40.
116. Franks W, Schenker I, Schmutz P, Hierlemann A. Impedance characterization and modeling of electrodes for biomedical applications. IEEE Trans Biomed Eng. 2005;52(7):1295–302.
117. Schaur S, Jakoby B, Kronreif G, IEEE. Position-dependent characterization of bone tissue with electrical impedance spectroscopy. In: 2012 IEEE sensors proceedings. IEEE: New York; 2012. p. 1352–5.
118. Sankar V, Patrick E, Dieme R, Sanchez J, Prasad A, Nishida T. Electrode impedance analysis of chronic tungsten microwire neural implants: understanding abiotic vs. biotic contributions. Front Neuroeng. 2014;7:13.
119. Nicholas LO, Sam EJ, Gil SR, Stephen MR, David BG, Anthony NB, Clive NM, Terence JOB, Thomas JO. Chronic impedance spectroscopy of an endovascular stent-electrode array. J Neural Eng. 2016;13(4):046020.
120. Moore Z, Patton D, Rhodes SL, O'Connor T. Subepidermal moisture (SEM) and bioimpedance: a literature review of a novel method for early detection of pressure-induced tissue damage (pressure ulcers). Int Wound J. 2017;14(2):331–7.
121. Clemente F, Romano M, Bifulco P, Cesarelli M. Study of muscular tissue in different physiological conditions using electrical impedance spectroscopy measurements. Biocybern Biomed Eng. 2014;34(1):4–9.
122. Okamoto E, Kikuchi S, Mitamura Y. Electrical characteristic of the titanium mesh electrode for transcutaneous intrabody communication to monitor implantable artificial organs. J Artif Organs. 2016;19(3):257–61.
123. Zhou XH, Zhang MK, Yu T, Liu YC, Shi HC. Oxygen profiles in biofilms undergoing endogenous respiration. Chem Eng J. 2013;220:452–8.
124. Clemente F, Costa M, Monini S, Barbara M. Monitoring of fixture osteointegration after BAHA (R) implantation. Audiol Neuro-Otol. 2011;16(3):158–63.
125. Teichmann D, Rohe L, Niesche A, Mueller M, Radermacher K, Leonhardt S. Estimation of penetrated bone layers during craniotomy via bioimpedance measurement. IEEE Trans Biomed Eng. 2017;64(4):765–74.
126. Balmer TW, Anso J, Muntane E, Gavaghan K, Weber S, Stahel A, Buchler P. In-vivo electrical impedance measurement in mastoid bone. Ann Biomed Eng. 2017;45(4):1122–32.
127. Collins PC, Paterson DC, Vernon-Roberts B, Pfeiffer D. Bone formation and impedance of electrical current flow. Clin Orthop Relat Res. 1981;155:196–210.
128. Gupta K, Gupta P, Singh G, Kumar S, Singh RK, Srivastava R. Changes in electrical properties of bones as a diagnostic tool for measurement of fracture healing. Hard Tissue. 2013;2:3.
129. Lin MC, Hu DE, Marmor M, Herfat ST, Bahney CS, Maharbiz MM. Smart bone plates can monitor fracture healing. Sci Rep. 2019;9:15.
130. Kozhevnikov E, Hou XL, Qiao SP, Zhao YF, Li CF, Tian WM. Electrical impedance spectroscopy: a potential method for the study and monitoring of a bone critical-size defect healing process treated with bone tissue engineering and regenerative medicine approaches. J Mater Chem B. 2016;4(16):2757–67.
131. Fox WC, Miller MA. Osseous implant for studies of biomaterials using an invivo electrochemical transducer. J Biomed Mater Res. 1993;27(6):763–73.
132. Cosoli G, Scalise L, Tricarico G, Russo P, Cerri G. Bioimpedance measurements in dentistry to detect inflammation: numerical modelling and experimental results. Physiol Meas. 2017;38(6):1145–57.
133. Duan YY, Clark GM, Cowan RSC. A study of intra-cochlear electrodes and tissue interface by electrochemical impedance methods in vivo. Biomaterials. 2004;25(17):3813–28.
134. Arpaia P, Clemente F, Romanucci C. An instrument for prosthesis osseointegration assessment by electrochemical impedance spectrum measurement. Measurement. 2008;41(9):1040–4.
135. Sendi P, Zimmerli W. Diagnosis of periprosthetic joint infections in clinical practice. Int J Artif Organs. 2012;35(10):913–22.

136. Ward AC, Tucker NP, Connolly P, IEEE. Development of a diagnostic device to detect different Pseudomonas aeruginosa phenotypes in medically relevant contexts. In: 2014 36th annual international conference of the IEEE engineering in medicine and biology society. IEEE: New York; 2014. p. 2757–60.
137. Grossi M, Ricco B. Electrical impedance spectroscopy (EIS) for biological analysis and food characterization: a review. J Sens Sens Syst. 2017;6(2):303–25.
138. Farrow MJ, Hunter IS, Connolly P. Developing a real time sensing system to monitor bacteria in wound dressings. Biosensors. 2012;2(2):171–88.
139. Varshney M, Li Y. Interdigitated array microelectrodes based impedance biosensors for detection of bacterial cells. Biosens Bioelectron. 2009;24(10):2951–60.
140. Kim S, Yu G, Kim T, Shin K, Yoon J. Rapid bacterial detection with an interdigitated array electrode by electrochemical impedance spectroscopy. Electrochim Acta. 2012;82:126–31.
141. Paredes J, Becerro S, Arizti F, Aguinaga A, Del Pozo JL, Arana S. Interdigitated microelectrode biosensor for bacterial biofilm growth monitoring by impedance spectroscopy technique in 96-well microtiter plates. Sens Actuators B Chem. 2013;178:663–70.
142. Paredes J, Alonso-Arce M, Schmidt C, Valderas D, Sedano B, Legarda J, Arizti F, Gómez E, Aguinaga A, Del Pozo JL, Arana S. Smart central venous port for early detection of bacterial biofilm related infections. Biomed Microdevice. 2014;16(3):365–74.
143. Paredes J, Becerro S, Arizti F, Aguinaga A, Del Pozo JL, Arana S. Real time monitoring of the impedance characteristics of Staphylococcal bacterial biofilm cultures with a modified CDC reactor system. Biosens Bioelectron. 2012;38(1):226–32.
144. Furst AL, Francis MB. Impedance-based detection of bacteria. Chem Rev. 2019;119(1):700–26.
145. Amiri M, Bezaatpour A, Jafari H, Boukherroub R, Szunerits S. Electrochemical methodologies for the detection of pathogens. ACS Sens. 2018;3(6):1069–86.
146. Hoyos-Nogues M, Brosel-Oliu S, Abramova N, Munoz FX, Bratov A, Mas-Moruno C, Gil FJ. Impedimetric antimicrobial peptide-based sensor for the early detection of periodontopathogenic bacteria. Biosens Bioelectron. 2016;86:377–85.
147. Ahmed A, Rushworth JV, Wright JD, Millner PA. Novel impedimetric irnmunosensor for detection of pathogenic bacteria *Streptococcus pyogenes* in human saliva. Anal Chem. 2013;85(24):12118–25.
148. Farrow MJ, Hunter I, Connolly P. Developing a real time sensing system to monitor bacteria in wound dressings. Biosensors. 2012;2:171–88.
149. Russell C, Ward AC, Vezza V, Hoskisson P, Alcorn D, Steenson DP, Corrigan DK. Development of a needle shaped microelectrode for electrochemical detection of the sepsis biomarker interleukin-6 (IL-6) in real time. Biosens Bioelectron. 2019;126:806–14.